UNIVERSITY OF THESSALY

DEPARTMENT OF MECHANICAL & INDUSTRIAL ENGINEERING

Master of Science Thesis

STABILITY OF CONFINED TWIN-WALLED STEEL CYLINDERS UNDER EXTERNAL PRESSURE

Daniel Vasilikis

Diploma in Mechanical and Industrial Engineering, University of Thessaly, 2006

ADVISOR PROFESSOR: S. A. KARAMANOS

A Thesis Submitted in Partial Fulfillment
of the Requirements for the Degree
of Master of Science

Volos, February 2008

ΠΑΝΕΠΙΣΤΗΜΙΟ ΘΕΣΣΑΛΙΑΣ

ΠΟΛΥΤΕΧΝΙΚΗ ΣΧΟΛΗ

ΤΜΗΜΑ ΜΗΧΑΝΟΛΟΓΩΝ ΜΗΧΑΝΙΚΩΝ ΒΙΟΜΗΧΑΝΙΑΣ

Μεταπτυχιακή Εργασία

ΕΥΣΤΑΘΕΙΑ ΕΓΚΙΒΩΤΙΣΜΕΝΩΝ ΛΕΠΤΟΤΟΙΧΩΝ ΜΕΤΑΛΛΙΚΩΝ ΚΥΛΙΝΔΡΩΝ ΥΠΟ ΕΞΩΤΕΡΙΚΗ ΠΙΕΣΗ

Δανιήλ Βασιλικής

Διπλωματούχος Μηχανολόγος Μηχανικός Π.Θ., 2006

ΕΠΙΒΛΕΠΩΝ ΚΑΘΗΓΗΤΗΣ: Σ. Α. ΚΑΡΑΜΑΝΟΣ

Υπεβλήθη για την εκπλήρωση μέρους των
απαιτήσεων για την απόκτηση του
Μεταπτυχιακού Διπλώματος Ειδίκευσης

Βόλος, Φεβρουάριος 2008

Η έγκριση της μεταπτυχιακής εργασίας από το Τμήμα Μηχανολόγων Μηχανικών Βιομηχανίας της Πολυτεχνικής Σχολής του Πανεπιστημίου Θεσσαλίας δεν υποδηλώνει αποδοχή των απόψεων του συγγραφέα (Ν. 5343/32 αρ. 202 παρ. 2).

Εγκρίθηκε από τα Μέλη της Πενταμελούς Εξεταστικής Επιτροπής:

Πρώτος Εξεταστής (Επιβλέπων)	Δρ. Σπύρος Α. Καραμάνος Επίκουρος Καθηγητής, Τμήμα Μηχανολόγων Μηχανικών Βιομηχανίας, Πανεπιστήμιο Θεσσαλίας
Δεύτερος Εξεταστής	Δρ. Νικόλαος Αράβας Καθηγητής, Τμήμα Μηχανολόγων Μηχανικών Βιομηχανίας, Πανεπιστήμιο Θεσσαλίας
Τρίτος Εξεταστής	Δρ. Γρηγόρης Χαϊδεμενόπουλος Καθηγητής, Τμήμα Μηχανολόγων Μηχανικών Βιομηχανίας, Πανεπιστήμιο Θεσσαλίας
Τέταρτος Εξεταστής	Δρ. Αλέξιος Κερμανίδης Λέκτορας, Τμήμα Μηχανολόγων Μηχανικών Βιομηχανίας, Πανεπιστήμιο Θεσσαλίας
Πέμπτος Εξεταστής	Δρ. Παναγιώτης Ντακούλας Αναπληρωτής Καθηγητής, Τμήμα Πολιτικών Μηχανικών, Πανεπιστήμιο Θεσσαλίας

ΕΥΧΑΡΙΣΤΙΕΣ

Πρώτα απ' όλα θα ήθελα να ευχαριστήσω τον επιβλέποντα της μεταπτυχιακής μου εργασίας, Επίκουρο Καθηγητή κ. Σπύρο Καραμάνο, για την καθημερινή ενασχόληση, την ουσιαστική καθοδήγηση και την πολύτιμη βοήθεια του καθ' όλη τη διάρκεια της μεταπτυχιακής εργασίας. Τον ευχαριστώ επίσης για τις πολύτιμες γνώσεις και συμβουλές του σε ακαδημαϊκά και όχι μόνο θέματα καθ' όλη τη διάρκεια της συνεργασίας μας. Πάνω απ' όλα όμως, τον ευχαριστώ για την εμπιστοσύνη που μου επιδεικνύει.

Επίσης είμαι ευγνώμων στους καθηγητές του τμήματος, Καθηγητή κ. Νικόλαο Αράβα και Καθηγητή κ. Γρηγόρη Χαϊδεμενόπουλο για τη γνώση που μου παρείχαν τόσο σε προπτυχιακό όσο και σε μεταπτυχιακό επίπεδο. Ευχαριστώ επίσης τον Λέκτορα κ. Αλέξη Κερμανίδη για την προσεκτική ανάγνωση της εργασίας, όπως επίσης και τον Αναπληρωτή Καθηγητή του τμήματος Πολιτικών Μηχανικών κ. Παναγιώτη Ντακούλα για την βοήθεια του στο πρόγραμμα πεπερασμένων στοιχείων Abaqus καθώς και για τις πολύτιμες υποδείξεις και παρατηρήσεις του.

Θα ήθελα να ευχαριστήσω θερμά τους Υποψήφιους Διδάκτορες του τμήματος κα. Σωτηρία Χουλιαρά, κα. Πατρικία Παππά και κο. Γιώργο Βαρέλη για την εποικοδομητική συνύπαρξη στο Εργαστήριο Μηχανικής και Αντοχής των Υλικών, για την υπομονή τους καθώς και για τη γενικότερη βοήθεια που μου προσέφεραν. Ευχαριστώ επίσης την κα. Ιωάννα Χαραλάμπους για την γραμματειακή υποστήριξη.

Στο σημείο αυτό θα ήθελα να ευχαριστήσω ολόψυχα τους φίλους μου Γιάννη Νικολάου, Ματούλα Μιχαλάκη και Πατρίτσια Παππά για τις στιγμές που περάσαμε μαζί όλα αυτά τα χρόνια στο Βόλο, για το γεγονός ότι τους ένιωθα πάντοτε δίπλα μου, για την αγάπη τους και για την συμπαράσταση τους.

Πάνω απ' όλα όμως, θα ήθελα να ευχαριστήσω την οικογένεια μου για την ηθική και οικονομική υποστήριξη που μου παρείχαν σε όλη τη διάρκεια των σπουδών μου. Η συνεχής συμπαράσταση τους και η εμπιστοσύνη που μου έδειχναν αποτέλεσε το βασικότερο κίνητρο μου και συνέβαλε καθοριστικά ώστε να βρίσκομαι σήμερα σ' αυτό το σημείο. Τους ευχαριστώ κυρίως, γιατί το δικό τους όνειρο για την ολοκλήρωση των σπουδών μου, αποτελεί πλέον δική μου κληρονομιά. Ως ελάχιστο δείγμα ευγνωμοσύνης, τους αφιερώνω την παρούσα εργασία.

Δανιήλ Βασιλικής

ΕΥΣΤΑΘΕΙΑ ΕΓΚΙΒΩΤΙΣΜΕΝΩΝ ΛΕΠΤΟΤΟΙΧΩΝ ΜΕΤΑΛΛΙΚΩΝ ΚΥΛΙΝΔΡΩΝ ΥΠΟ ΕΞΩΤΕΡΙΚΗ ΠΙΕΣΗ

Δανιήλ Βασιλικής

Πανεπιστήμιο Θεσσαλίας, Τμήμα Μηχανολόγων Μηχανικών Βιομηχανίας, 2008

Επιβλέπων Καθηγητής: Δρ. Σπύρος Α. Καραμάνος, Επίκουρος Καθηγητής

Περίληψη

Στην παρούσα εργασία μελετάται η δομική ευστάθεια των λεπτότοιχων μεταλλικών κυλίνδρων που περιβάλλονται από ένα ελαστικό μέσο και οι οποίοι υπόκεινται σε ομοιόμορφη εξωτερική πίεση. Για την μελέτη αυτή αναπτύχθηκε ένα διδιάστατο μοντέλο, υποθέτοντας ότι το φορτίο και η παραμόρφωση δεν μεταβάλλονται κατά μήκος του κυλίνδρου. Ο κύλινδρος και το περιβάλλον μέσο προσομοιώθηκαν με μη-γραμμικά πεπερασμένα στοιχεία λαμβάνοντας υπόψη τη μη-γραμμικότητα γεωμετρίας και υλικού. Αρχικά μελετήθηκαν κύλινδροι από ελαστικό υλικό, οι οποίοι περιβάλλονται από ένα άκαμπτο (απαραμόρφωτο) μέσο, και τα αποτελέσματα της ανάλυσης αυτής επιβεβαιώθηκαν με διαθέσιμες αναλυτικές λύσεις. Στη συνέχεια εξετάστηκε η απόκριση των εγκιβωτισμένων λεπτότοιχων μεταλλικών κυλίνδρων σε εξωτερική πίεση, για διάφορες τιμές της αρχικής ατέλειας του κυλίνδρου, του κενού μεταξύ κυλίνδρου και μέσου και της ακαμψίας του μέσου. Τα αποτελέσματα της ανάλυσης παρουσιάζονται σε διαγράμματα δρόμου ισορροπίας πίεσης-μετατόπισης, στα οποία παρατηρείται μια ραγδαία πτώση της αντοχής μετά το σημείο της μέγιστης πίεσης που μπορεί να παραλάβει ο κύλινδρος. Επίσης μελετάται η κατανομή της πλαστικής παραμόρφωσης καθώς και η μεταβολή της πίεσης επαφής κυλίνδρου-μέσου κατά την περιφέρεια του κυλίνδρου. Ακόμα εξετάζεται η επίδραση της επιβολής κάθετης ομοιόμορφης προφόρτισης στην μέγιστη πίεση που μπορεί να παραλάβει ο κύλινδρος χωρίς να αστοχήσει. Τέλος, τα αποτελέσματα της ανάλυσης συγκρίνονται με μια απλοποιημένη έκφραση που έχει προταθεί παλαιότερα και η οποία θα μπορούσε να χρησιμοποιηθεί για το σχεδιασμό τέτοιων κατασκευών.

STABILITY OF CONFINED TWIN-WALLED STEEL CYLINDERS UNDER EXTERNAL PRESSURE

Daniel Vasilikis

University of Thessaly, Department of Mechanical & Industrial Engineering, 2008

Advisor Professor: Dr. Spyros A. Karamanos, Assistant Professor

Abstract

The present thesis investigates the structural stability of thin-walled steel cylinders surrounded by an elastic medium, subjected to uniform external pressure. A two dimensional model is developed, assuming no variation of load and deformation along the cylinder axis. The cylinder and the surrounding medium are simulated with nonlinear finite elements that account for both geometric and material nonlinearities. Cylinders of elastic material within a rigid boundary are considered first, and the numerical results are compared successfully with available closed-form analytical predictions. Subsequently, the external pressure response of confined thin-walled steel cylinders is examined, in terms of initial out-of-roundness of the cylinder, initial gap between the cylinder and the medium and the stiffness of the medium. Numerical results are presented in the form of pressure-deflection equilibrium paths, which show a rapid drop of pressure capacity after reaching the maximum pressure level. The distribution of plastic deformation, as well as the variation of cylinder-medium contact pressure around the cylinder cross-section are also depicted and discussed. Furthermore, the effects of uniform vertical preloading on the maximum pressure sustained by the cylinder are examined. Finally, the numerical results are compared with a simplified closed-form expression, proposed elsewhere, that could be used for design purposes.

CONTENTS

CHAPTER 1

INTRODUCTION

Twin-walled elastic cylinders, when subjected to uniform external hydrostatic pressure, under unconfined lateral conditions, buckle in the elastic range in the form of an oval shape. Assuming isotropic elastic behavior, the corresponding critical pressure p_{cr} is equal to [1]

$$p_{cr} = \frac{2E}{1-\nu^2}\left(\frac{t}{D}\right)^3 \tag{1.1}$$

where E is the Young's modulus, ν is Poisson's ratio, D is the cylinder diameter and t is the wall thickness. The above elastic critical pressure is valid for steel cylinders with diameter-to-thickness ratio greater than about 40, and it is well below the yield pressure p_y, i.e. the pressure that causes full plastification of the cylinder. From thin-walled vessel theory, and considering a von Mises yield criterion, this plastic pressure p_y is readily calculated equal to

$$p_y = 2\frac{\sigma_y}{\sqrt{1-\nu+\nu^2}}\left(\frac{t}{D}\right) \tag{1.2}$$

where σ_y is the yield stress of the material under uniaxial stress conditions, and factor $1/\sqrt{1-\nu+\nu^2}$ accounts for increase of yield stress in the hoop direction due to plane strain conditions. Assuming $\nu = 0.30$ for metals, this factor is equal to 1.13. Variations of the elastic buckling pressure formula (1.1), have been widely used for the design of relatively thin-walled offshore pipes and tubulars, accounting for initial imperfections and residual stresses [2], [3] and [4].

In several engineering applications, steel cylinders subjected to external pressure are confined within a surrounding medium. Under those conditions, the cylinder may buckle because of excessive hoop compression. Buried steel pipelines [5], and steel liners, used to rehabilitate damaged pipelines [6], are typical examples. Furthermore, tunnels and ducts that transport gases or liquids in power plants are often lined with cylindrical steel shells [7]. Finally, steel cylinders are also employed as casing in oil and gas production wells [8]. In all the above applications, significant hoop stresses develop in the cylinder wall due to either thermal effects or hydrostatic pressure conditions because of ground water and the permeability of the surrounding medium. When these hoop stresses exceed a critical level, the steel cylinder buckles. However, in such a case, due to the surrounding medium, the steel cylinder is not free to deform outwards and the critical pressure of equation (1.1) is no longer applicable. Buckling occurs in the form of an "inward lobe", as shown in Figure 1 at a pressure level significantly higher than the one predicted by equation (1.1).

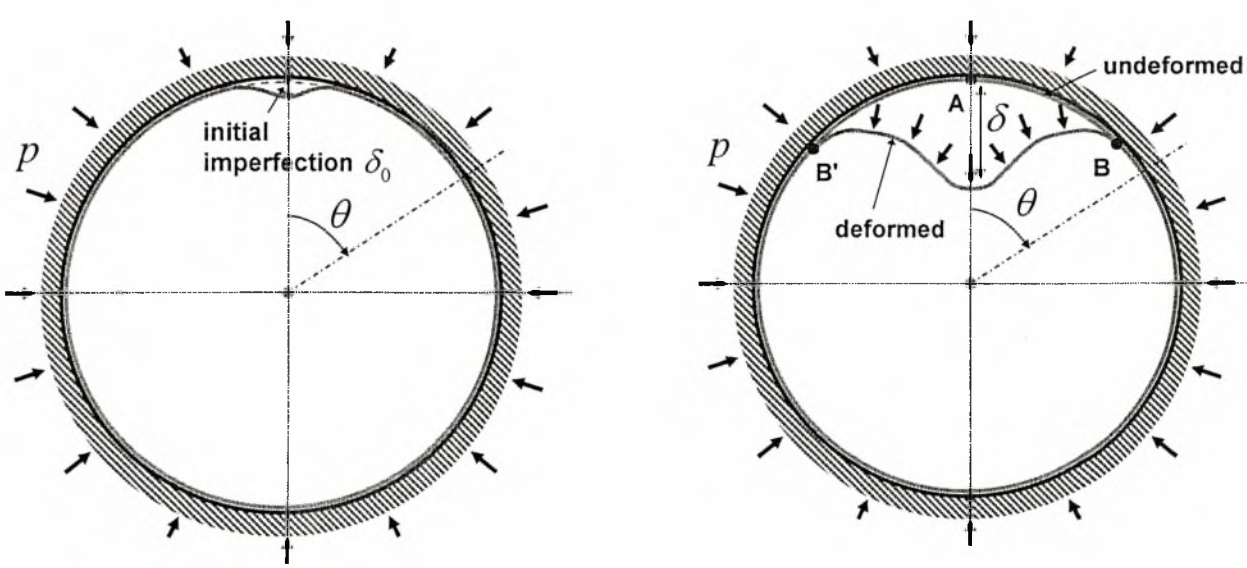

Figure 1 Schematic representation of a confined ring under uniform external pressure.

The present work, motivated by the structural response of buried pipelines surrounded by saturated soil medium or concrete encasement, focuses on buckling of confined cylinders under external hydrostatic pressure. When the groundwater table is above the pipeline level, the water reaches the pipe through the permeable surrounding soil or concrete and hydrostatic pressure conditions develop around the pipeline, which may cause buckling of the steel pipeline wall. It should be noted that buckling under hydrostatic pressure is quite different than buckling under thermal effects, sometimes referred to as "shrink buckling" [9], [10], [11], [12] and [13]. In "shrink buckling", hoop compressive force is relieved immediately after buckling occurs, whereas in hydrostatic buckling, pressure load is always present in the post-buckling stage. For an extensive literature review on the "shrink buckling" problem, the reader is referred to the paper by Omara et al. [6].

Hydrostatic buckling of elastic cylinders embedded in a stiff medium has been examined by Cheney [14] through an energy approach. The ring was considered to consist of two portions, the "buckle portion" and the "unbuckled" portion, as shown in Figure 1. Cheney further assumed that the cavity may move inward with the ring, resisting outward movement of the ring wall, but not its inward displacement. Minimization of the potential energy and solution of the corresponding differential equations, with appropriate boundary conditions, resulted in the following expression for the critical pressure:

$$p_{CH} = 2.55\frac{E}{1-\nu^2}\left(\frac{t}{D}\right)^{2.2} \tag{1.3}$$

Glock [15] presented an energy formulation and solution of the hydrostatic buckling problem of elastic cylinders, assuming no friction between the ring and the stiff medium. It was further assumed that the cavity does not move inwards with the

ring. Minimization of the potential energy and assuming a constant hoop membrane force around the cylinder cross-section, resulted in the following expression for the buckling pressure:

$$p_{GL} = \frac{E}{1-\nu^2}\left(\frac{t}{D}\right)^{2.2} \tag{1.4}$$

A brief presentation of this analytical solution is offered in the Appendix. Comparisons with experimental data, as well as with nonlinear finite element results [16] indicated that Glock's formula (1.4) can predict quite accurately the buckling pressure of tightly-fitted elastic cylinders. Furthermore, based on their numerical results and accounting for the presence of initial gap between the cylinder [see Figure 2 (b) in Chapter 2] and the rigid surrounding medium, El-Sawy and Moore [16] proposed the following empirical analytical expression for the buckling pressure of elastic cylinders:

$$p_{EM} = \frac{2E}{1-\nu^2}\left(\frac{t}{D}\right)^3\left(\frac{25+700(t/D)+315(g/R)}{0.15+130(t/D)+1400(t/D)^2+145(g/R)}\right) \tag{1.5}$$

The last term within the parenthesis in the right-hand side of above equation express the increase of the classical elastic formula for unconfined conditions [equation (1.1)] when rigid confining conditions are imposed on the externally pressurized cylinder. In a later publication, Boot [17] enhanced Glock's solution [15] to account for the presence of initial gap between the cylinder and the stiff surrounding medium, and reported implicit analytical expressions for the buckling pressure.

The above works on confined cylinder buckling refer to cylinders with elastic material behaviour. Compared with the numerous publications on elastic cylinders, relatively few investigations exist on the corresponding buckling problem of steel cylinders, which is associated with elastic-plastic material behaviour. As a first approximation, the ultimate external pressure capacity can be estimated as the pressure

that causes first yielding at the outer fibre of the cylinder wall. Adopting this concept, Montel [18] used Timoshenko's solution for thin ring deflection [see [19]] and experimental data to develop a semi-empirical formula for the buckling pressure of cylinders embedded in a stiff boundary, in terms of the material yield stress σ_y and the cylinder geometry R/t, initial imperfection δ_0 and initial gap g between the cylinder and the stiff boundary:

$$p_M = \frac{5\sigma_y}{(R/t)^{1.5}\left[1+1.2(\delta_0+2g)/t\right]} \tag{1.6}$$

Montel [18] proposed the above equation (1.6) for $30 \le R/t \le 170$, $250\ MPa \le \sigma_y \le 500\ MPa$, $0.1 \le \delta_0/t \le 0.5$, $g/t \le 0.25$ and $g/R \le 0.025$.

Using a two-dimensional model and assuming first-yielding failure, Amstutz [20] developed a formula for the external pressure collapse of embedded rings, which has been widely used for design purposes. The problem was also investigated by Jacobsen [21], assuming failure at first yielding. Jacobsen, accounting for the presence of gap between the cylinder and the rigid medium, and considering a cosine function to describe the single-lobe buckling shape, resulted in implicit analytical expressions for the ultimate external pressure. A numerical solution for the ultimate pressure sustained by a steel cylinder embedded in a rigid cavity was reported by Yamamoto & Matsubara [22], using elastic-plastic ring analysis through beam finite elements and assuming a uniform gap between the steel ring and the confining medium. The importance of material nonlinearity on the cylinder response was noted, and an empirical formula, valid for low-strength steel ($\sigma_y = 235\ MPa$) that fits well with the finite element results, was developed through curve fitting.

A more rigorous investigation of buckling and post-buckling behaviour of confined cylinders under external pressure, was conducted by Kyriakides & Youn [23]

using a semi-analytical formulation, based on nonlinear ring theory. The cylinder was assumed inextensional in the hoop direction, and elastic-plastic behaviour was modelled through a bilinear material curve. The results in [23] have been used to study buckle propagation in confined long metal pipes [24] and [25]. Motivated by the structural design of rehabilitation metal liners, El-Sawy [26] and [27] examined numerically the buckling response of loosely-fitted and tightly-fitted cylinders respectively, surrounded by a rigid boundary and subjected to external pressure. Parametric studies in terms of yield stress σ_y and diameter-to-thickness ratio D/t have been conducted, accounting for the initial gap between the cylinder and the surrounding stiff boundary, and the numerical results were compared with the analytical results of Jacobsen [21]. An empirical equation showing the border between elastic and plastic buckling has also been proposed.

The present work, motivated by the structural behaviour of buried pipelines, focuses on the structural stability of steel cylinders confined by a deformable medium under uniform external pressure. The cylinders are thin-walled with diameter-to-thickness ratio (D/t) that ranges between 100 and 300, which is typical for water pipelines or rehabilitation liners, which may fail under external pressure (vacuum) conditions in a "single-lobe" shape. Assuming constant pressure around the pipe, and no variation of stress and deformation in the axial direction of the pipeline, a two-dimensional idealized problem under plane strain conditions is considered. Both the cylinder and the medium are modelled using finite elements, which account for inelastic effects and large deformations. The analysis is aimed primarily at tracing the pressure-displacement equilibrium path, and determining the maximum pressure sustained by the cylinder for different values of D/t ratio and yield stress of steel material. The sensitivity of buckling behaviour with respect to initial imperfections of the ring

geometry and the presence of a small gap between the ring and the medium are investigated. Furthermore, the effects of elastic medium modulus E' on the buckling response, as well as the influence of preloading on the top of the medium are examined. Finally, the present finite element results are compared with available analytical results [15],[16] and [18], towards better understanding of confined cylinder behaviour.

CHAPTER 2

FINITE ELEMENT SIMULATION

The response of confined cylinders under uniform external pressure is examined numerically using nonlinear finite element tools. General-purpose finite element program ABAQUS [28] is employed to simulate the buckling response of pressurized confined cylinders. The analysis considers nonlinear geometry through a large-strain description of the deformable continuum, as well as inelastic material behavior, accounted for through a J_2 flow (von Mises) large-strain plasticity model, with isotropic hardening.

Assuming no variation of loading and deformation in the longitudinal direction, the finite element model is two-dimensional, considering a strip of the cylinder under plain-strain conditions. Because of the symmetry of the single-lobe post-buckling shape of the cylinder, half of the cylinder cross-section is analyzed, applying appropriate symmetry conditions at the $\theta = 0, \pi$ plane. Four-node reduced-integration shell elements (type S4R) are employed for modeling of the pipe, whereas eight-node brick elements (type C3D8R) are used to simulate the surrounding medium. A typical finite element mesh for the elastic medium used in the present analyses is shown in Figure 2 (a). In this model, L and H are equal to 1.5 and 3 cylinder diameters respectively. Following a short parametric study, it has been concluded that consideration of a larger medium domain, and the use of a finer finite element mesh have negligible effect on the numerical results. Furthermore, a total of 150 shell elements around the cylinder half circumference have been found to be adequate to achieve convergence of solution and accuracy of the numerical results.

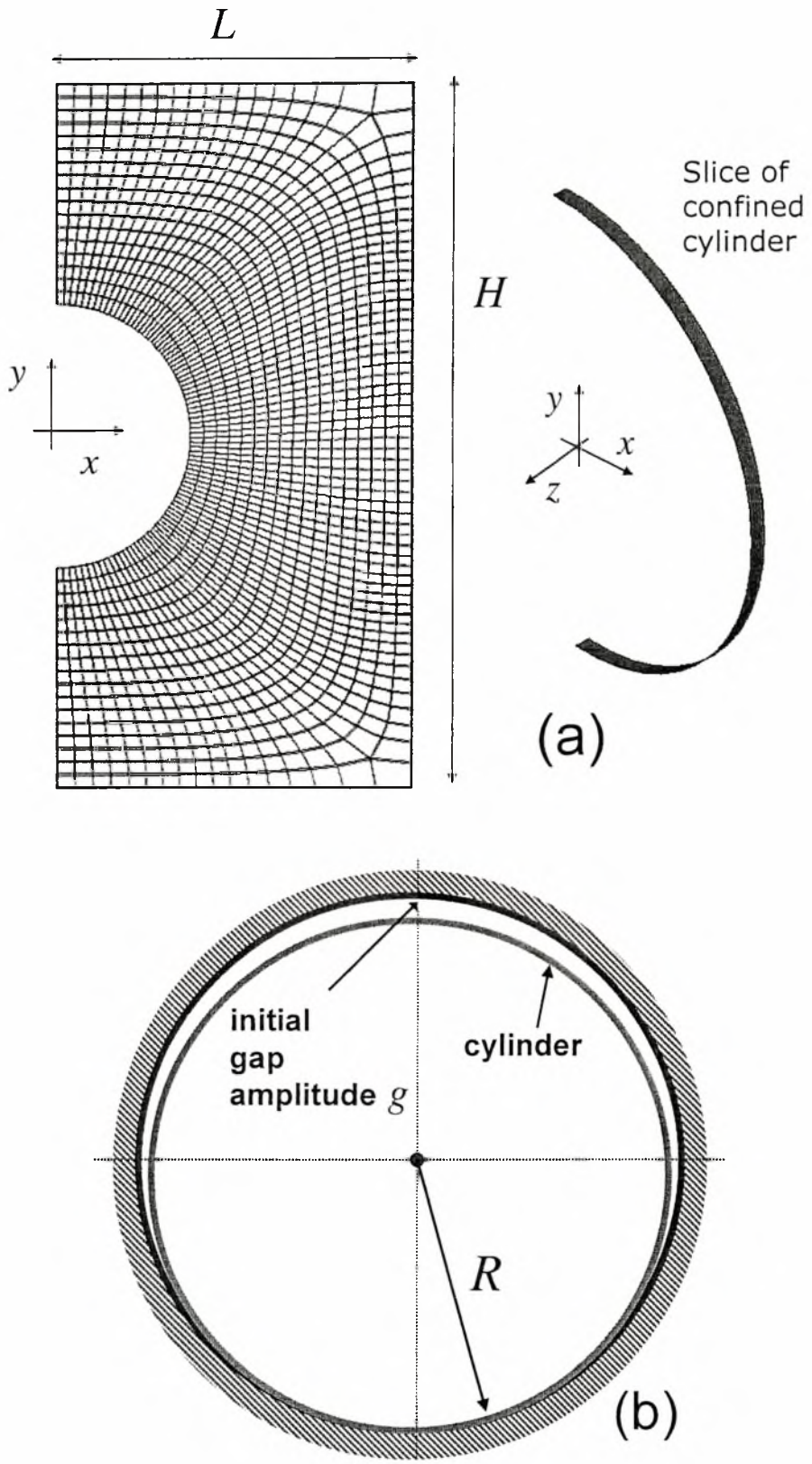

Figure 2 (a) Finite element model of embedded cylinder, (b) schematic representation of initial gap between the cylinder and the surrounding medium.

The model accounts for the presence of a gap between the medium and the steel cylinder. The gap is introduced in the model, assuming that the circular cavity of the medium has a radius slightly larger than the cylinder radius, and that the cylinder and the cavity are initially in contact at $\theta = \pi$. Therefore, the maximum gap between the cylinder and the medium occurs at $\theta = 0$, denoted as g, as shown in Figure 2 (b).

A contact algorithm is used to simulate the interface between the cylinder and the medium. In the most of the cases, contact is assumed frictionless. However, several analyses have been performed to examine the effects of friction, which is considered through the friction coefficient μ, where $\mu = \tan\phi$, and ϕ is the friction angle of the interface between the cylinder and the medium.

To perform the nonlinear analysis, enable the formation of single-lobe buckle and trace the post-buckling equilibrium path, a small initial imperfection on the cylinder is imposed. More specifically, small downward vertical load is applied at the $\theta = 0$ location, causing a localized displacement pattern. After the load is removed and despite the elastic rebound of the cylinder wall, the cylinder at this location contains a small residual displacement δ_0, which is considered as the initial imperfection (out-of-roundness). Subsequently, uniform external pressure is applied around the cylinder, and the nonlinear pressure-deflection $(p-\delta)$ equilibrium path is traced (where δ is the vertical displacememt of point A at $\theta = 0$), using a Riks continuation algorithm.

CHAPTER 3

NUMERICAL RESULTS FOR ELASTIC CYLINDERS

The response of thin-walled elastic cylinders with D/t values between 100 and 300, calculated through the finite element simulation, is examined first, and the response is compared with analytical solutions reported by Glock [15] and El-Sawy & Moore [16]. The material of the cylinder is considered elastic with a modulus E equal to 210,000 MPa and Poisson's ratio equal to 0.3. The modulus of the confinement medium E' has a value equal to 21,000 MPa (one-tenth of the steel material). Considering this value of E', the confinement medium is practically non-deformable and may be considered as rigid. A zero gap between the cylinder and the medium is assumed ($g/R=0$), as well as a negligible geometric initial imperfection ($\delta_0=0$). Finally, a frictionless interface is considered between the steel cylinder and the confinement medium.

The pressure-displacement curves are depicted in Figure 3 and show the equilibrium path of pressure p versus the vertical displacement δ of point A (Figure 1) at $\theta=0$, normalized by the tube radius R (δ/R). All equilibrium paths are characterized by a point of maximum (limit) pressure $p_{\max}$, beyond which, the cylinder exhibits a significant drop of pressure, indicating an unstable behavior. In all cases examined, the computed value of maximum (limit) pressure $p_{\max}$ is in excellent agreement with analytical predictions p_{GL} obtained by Glock [15] and p_{EM} obtained by El-Sawy & Moore [16], expressed through the simple closed-form expressions of equations (1.4) and (1.5), as shown in Figure 4.

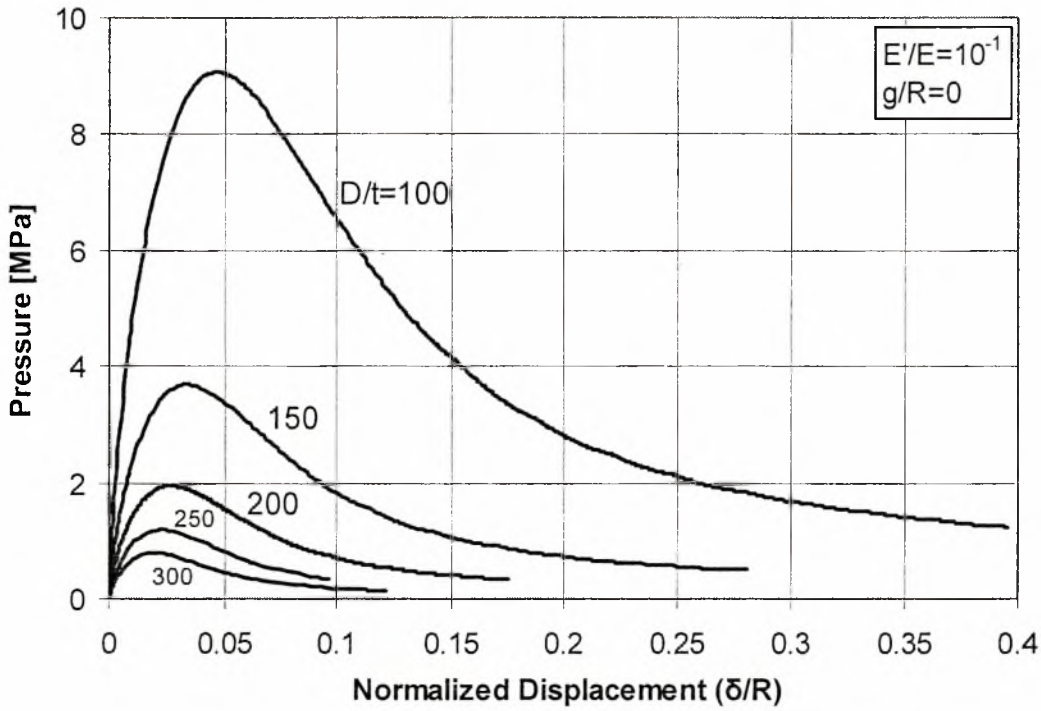

Figure 3 Response of tightly-fitted elastic cylinders embedded in a rigid confinement medium.

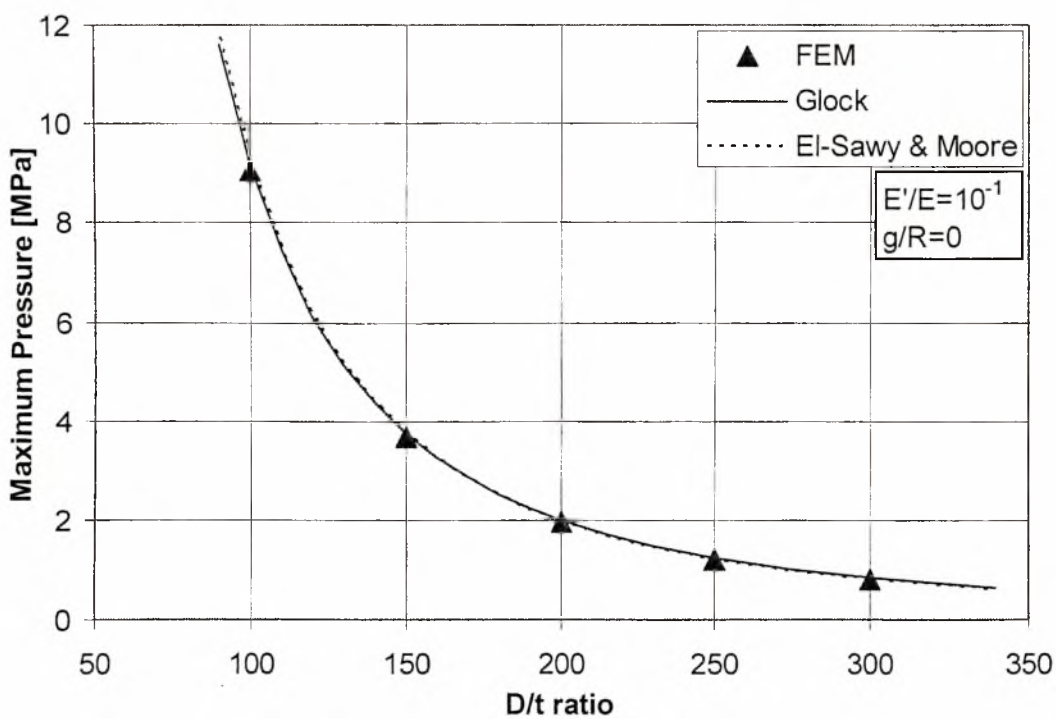

Figure 4 Comparison between numerical results and analytical predictions from Glock's equation [15] and El-Sawy & Moore equation [16] for the buckling pressure of rigidly confined cylinders.

Note that the value of maximum pressure p_{max} is 20 to 45 times larger than the value of the corresponding elastic buckling pressure p_e under unconfined conditions, expressed by equation (1.1). The large values of the p_{max}/p_e ratio express quantitively the very significant effect of confinement on the buckling resistance. Furthermore, the results offer a very good verification of the validity of Glock's analytical solution for elastic confined cylinders. It is interesting to note that Glock's equation and, therefore, the present finite element results are in close agreement with the experimental data reported in [29].

Consecutive deformation configurations of the cylinder under external pressure are shown in Figure 5 (left) and the corresponding points on the pressure-deflection path are depicted in Figure 5 (right). The numerical results indicate that the maximum pressure occurs at the stage where the local curvature at $\theta = 0$ becomes zero (i.e. when "inversion" of the cylinder wall occurs). This is in agreement with the analytical solution of Glock [15]. More specifically, using equations (1.3) and (1.4) of Appendix, the maximum local curvature k_0 at $\theta = 0$, is calculated as follows:

$$k_0 = \frac{w'(0)}{R^2} = -\frac{\delta}{2R^2}\left(\frac{\pi}{\phi}\right)^2 \tag{3.1}$$

Therefore, the curvature $k_{0,cr}$ at maximum pressure stage can be obtained analytically substituting equations (1.9) and (1.10) of Appendix into equation (3.1) to get

$$k_{0,cr} = -1.033\frac{1}{R} \simeq -\frac{1}{R} \tag{3.2}$$

The above analytical prediction indicates that the total instantaneous curvature at buckling at the $\theta = 0$ location is zero, i.e. inversion of the cylinder wall occurs, which is verified by the numerical results in Figure 5.

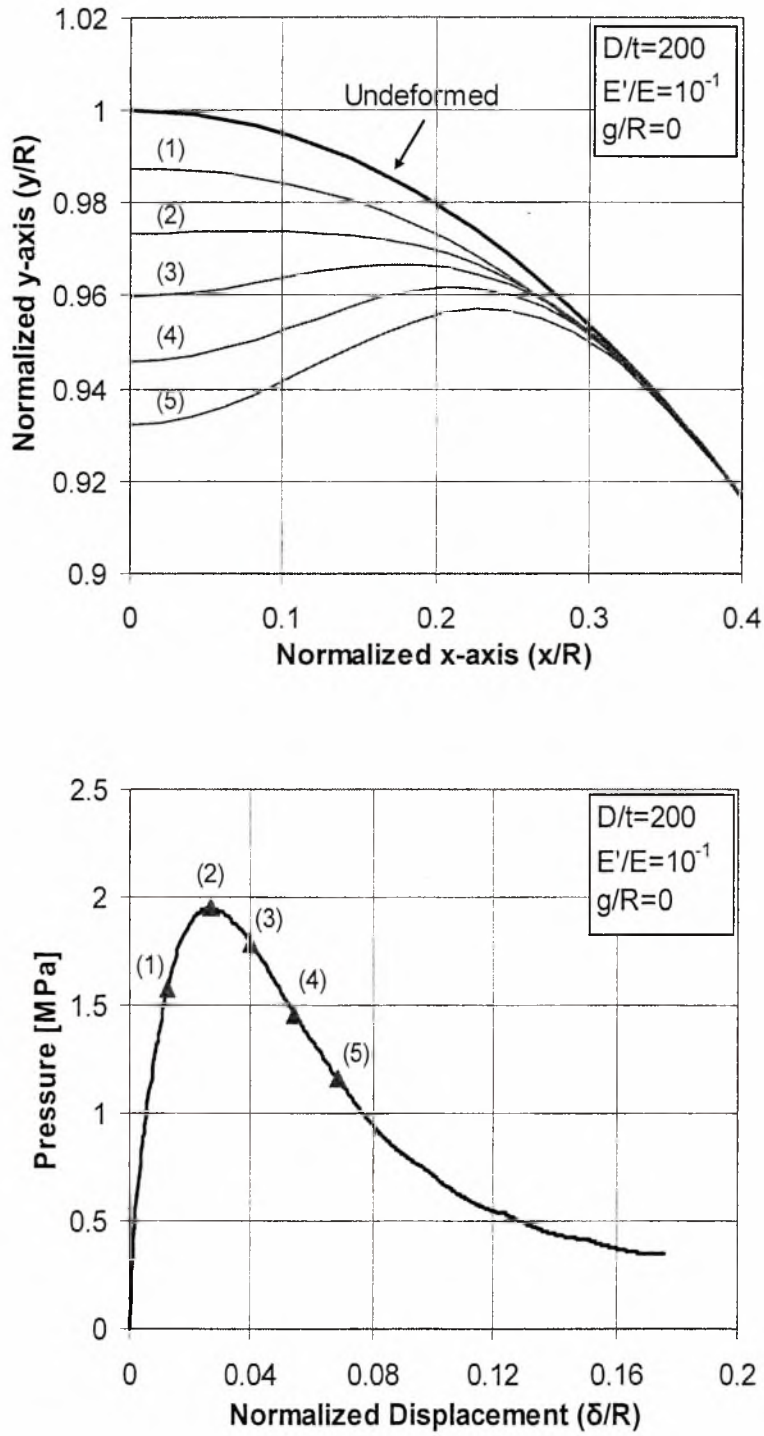

Figure 5 Consecutive deformation shapes of a tightly-fitted elastic cylinder; configuration (2) corresponds to ultimate pressure stage.

CHAPTER 4

NUMERICAL RESULTS FOR STEEL CYLINDERS

Using the above numerical models, the structural ability of externally-pressurized confined steel cylinders is examined, assuming an elastic confinement medium. The values of pressure p are normalized by the yield pressure $p_y = (2\times 1.13)\sigma_y t/D$ [see equation (1.2)], whereas the displacement δ of point A at $\theta = 0$ [see Figure 1] is normalized by the cylinder radius R.

The response of a thin-walled metal cylinder with $D/t = 200$ is shown in Figure 6, for different values of initial imperfection and assuming a frictionless interface between the cylinder and the confinement medium. The material of the cylinder is steel, with yield stress σ_y and ultimate stress σ_u equal to 313 MPa and 492 MPa respectively, whereas post-yield hardening is zero up to nominal strain equal to 1.5%. A zero gap between the cylinder and the medium, and a confinement medium modulus E' equal to 10% of E are assumed ($E' = 21{,}000MPa$). The value of E' corresponds to practically rigid confinement (e.g. concrete encasement). The equilibrium curves in Figure 6 represent the nonlinear relationship between the applied pressure and the downward displacement of the cylinder point at $\theta = 0$. The results indicate a significant sensitivity of the ultimate (maximum) pressure $p_{\max}$ sustained by the steel cylinder, with respect to the value of initial imperfection. It is also interesting to note that the value of the ultimate pressure $p_{\max}$ for negligible initial imperfection is substantially smaller than the yield pressure p_y.

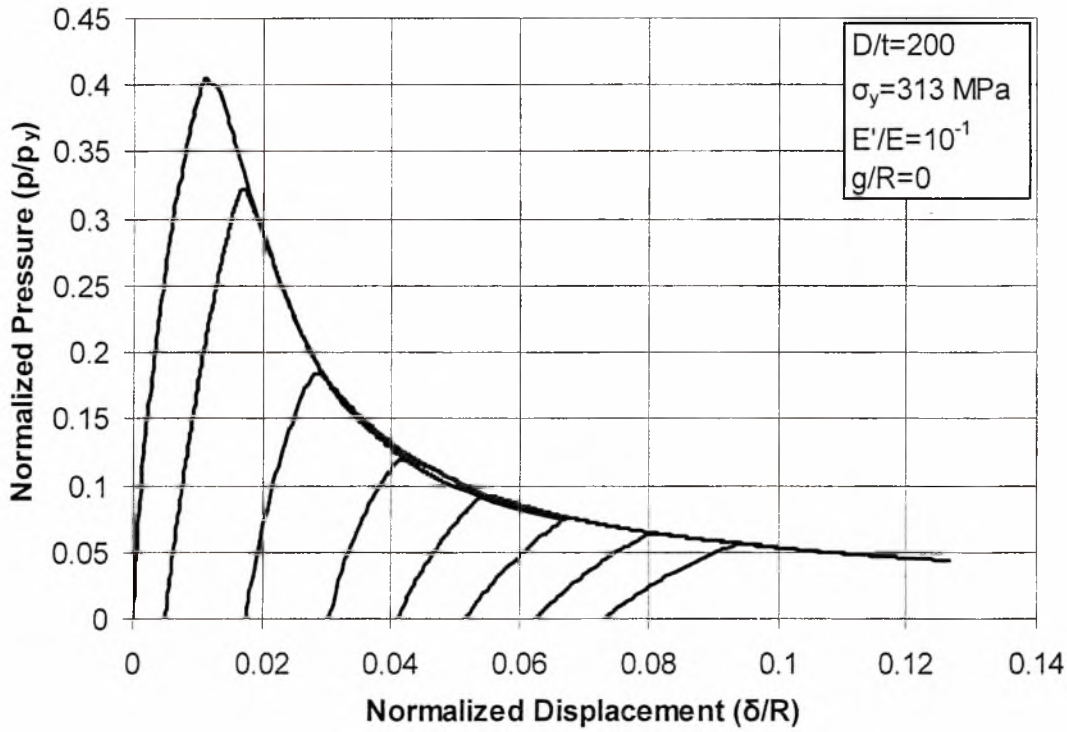

Figure 6 Response of tightly-fitted steel cylinders $(g/R=0)$, embedded in a rigid confinement medium $(D/t=200)$.

Comparison between the numerical results from the elastic case (Figure 3) and those shown in Figure 6 for steel cylinders shows that in steel cylinders, buckling of steel cylinder occurs at a lower level of pressure, indicating a significant effect of inelastic material behavior on the structural capacity of the cylinder under external pressure. Furthermore, the finite element results indicate that buckling of elastic-plastic (steel) cylinders occurs immediately after first yielding, which corresponds to a deformation stage before "inversion" of the cylinder wall occurs. In Figure 7 (a), the successive deformed configurations of the steel cylinder are depicted. A comparison between deformed shapes from elastic and inelastic cylinder behavior (Figure 7 (b)) that correspond to the same deflection of point A shows that the postbuckling shape of inelastic cylinders is characterized by more abrupt changes of local curvature at the

symmetry point A and the "touchdown" point B, and this is attributed to the concentration of plastic deformation at those points.

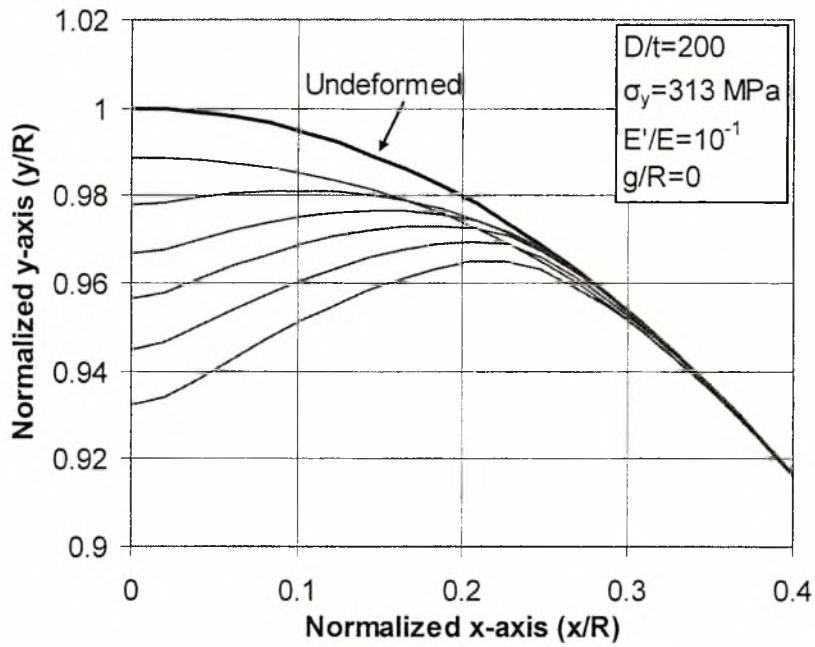

(a)

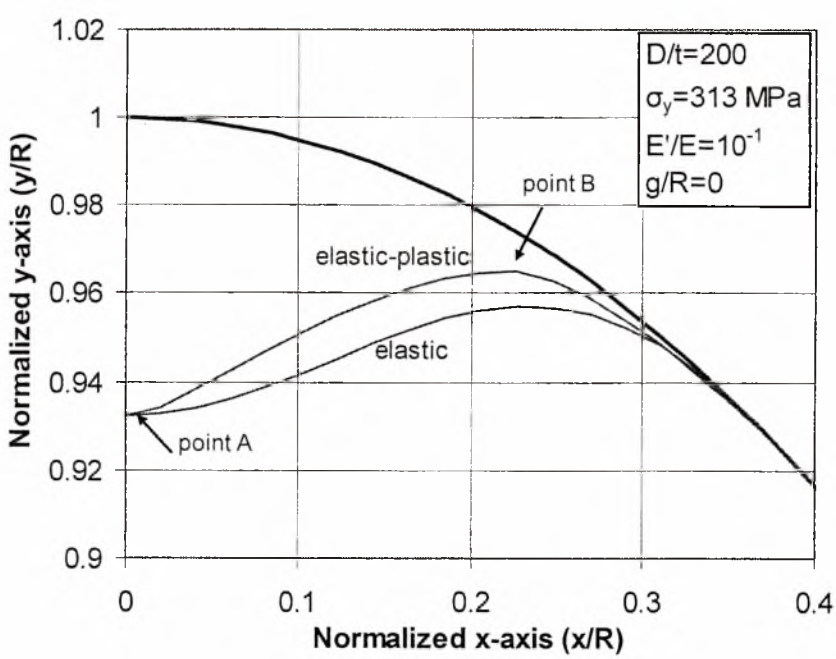

(b)

Figure 7 (a) Post-buckling shapes of tightly-fitted steel cylinders with elastic-plastic material; (b) comparison with corresponding stages of elastic cylinder.

Upon reaching the maximum pressure p_{max}, the cylinder behavior is unstable, characterized by a significant drop of pressure capacity. The reason for this unstable behavior is the formation of a plastic collapse mechanism with one stationary plastic hinge at symmetry point A, and two moving hinges at the two "touchdown" points B and B'. The distribution of plastic deformation along the cylinder perimeter is depicted in Figure 8 in terms of the equivalent plastic strain, indicating clearly plastic hinge

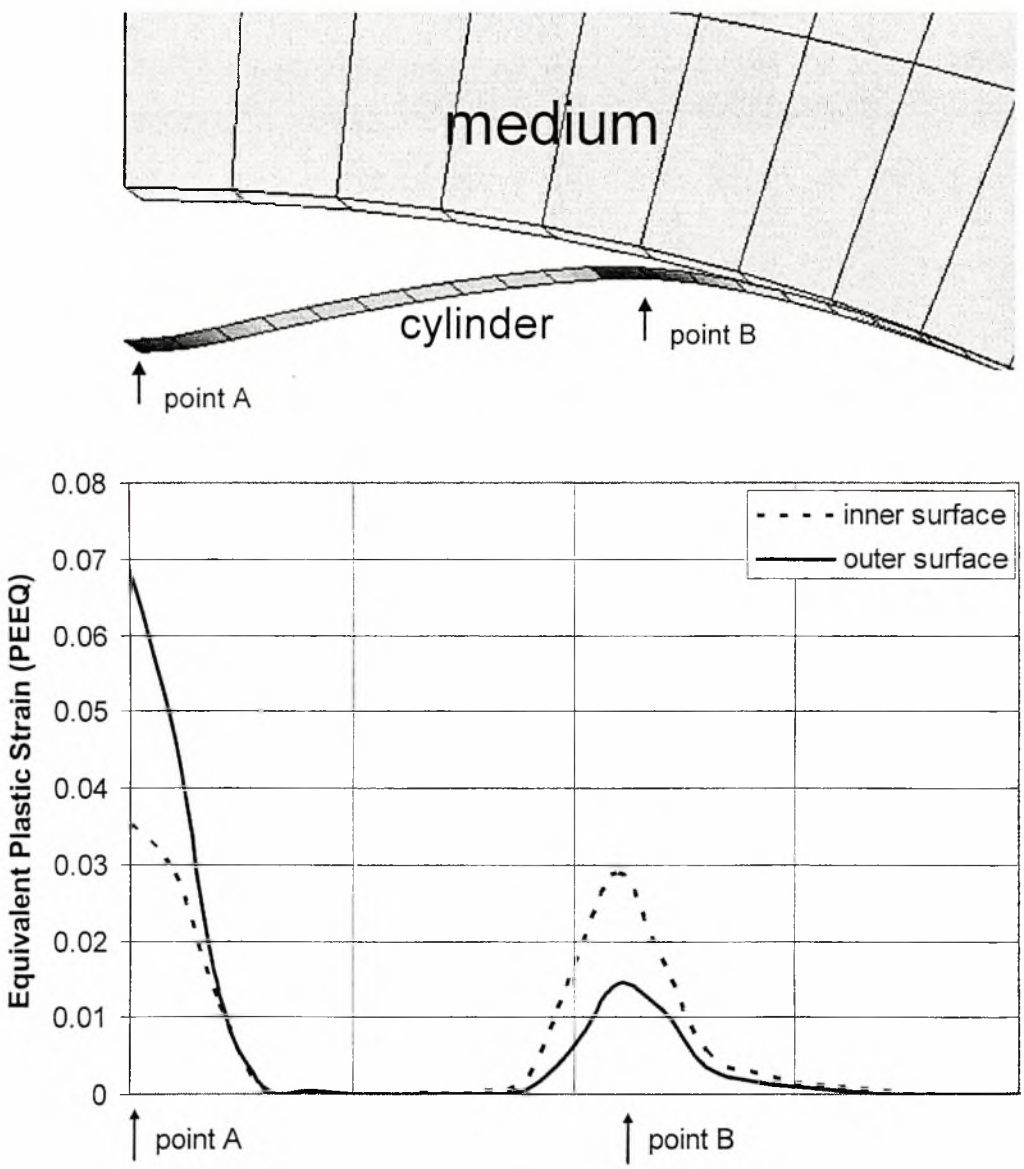

Figure 8 Distribution of plastic deformation, depicted in terms of equivalent plastic strain, along the pipe section in the buckled area ($E'/E = 10^{-1}$, $D/t = 200$).

formation at points A and B. The unstable postbuckling equilibrium path is responsible for a severe sensitivity of the maximum pressure value to the presence of initial imperfections. In Figure 6, the numerical results show that initial imperfections of amplitude less than 1% of the cylinder diameter result in a 60% reduction of the ultimate pressure $p_{\max}$.

The presence of a gap between the cylinder and the confinement medium may have significant effect on the maximum pressure, as shown in Figures 9. The cylinder has a D/t ratio equal to 200, and a steel material with yield stress σ_y equal to 313 MPa. The gap size, denoted as g, is the maximum distance between the cylinder and the medium at $\theta = 0$ [see Figure 2 (b) in Chapter 2], and it is normalized by the cylinder radius R. The numerical results in Figures 9, compared with the corresponding results of Figure 6, indicate that the presence of a rather small gap results in a reduction of the ultimate pressure capacity $p_{\max}$ of the cylinder. For zero initial imperfection, the ultimate capacity is reduced by 40% for an initial gap size equal to 0.27% of the cylinder radius R and by 64% for a gap size equal to 0.8% of the cylinder radius R. In both cases depicted in Figures 9, the response is sensitive to the presence of initial imperfections (δ_0/R). The effects of initial gap (g/R) and initial imperfections (δ_0/R) on the maximum pressure $(p_{\max}/p_y)$ are summarized in Figure 10. The finite element results indicate that for initial imperfection values δ_0 greater than 4% of the cylinder radius R the value of maximum pressure is independent of the value of initial gap g.

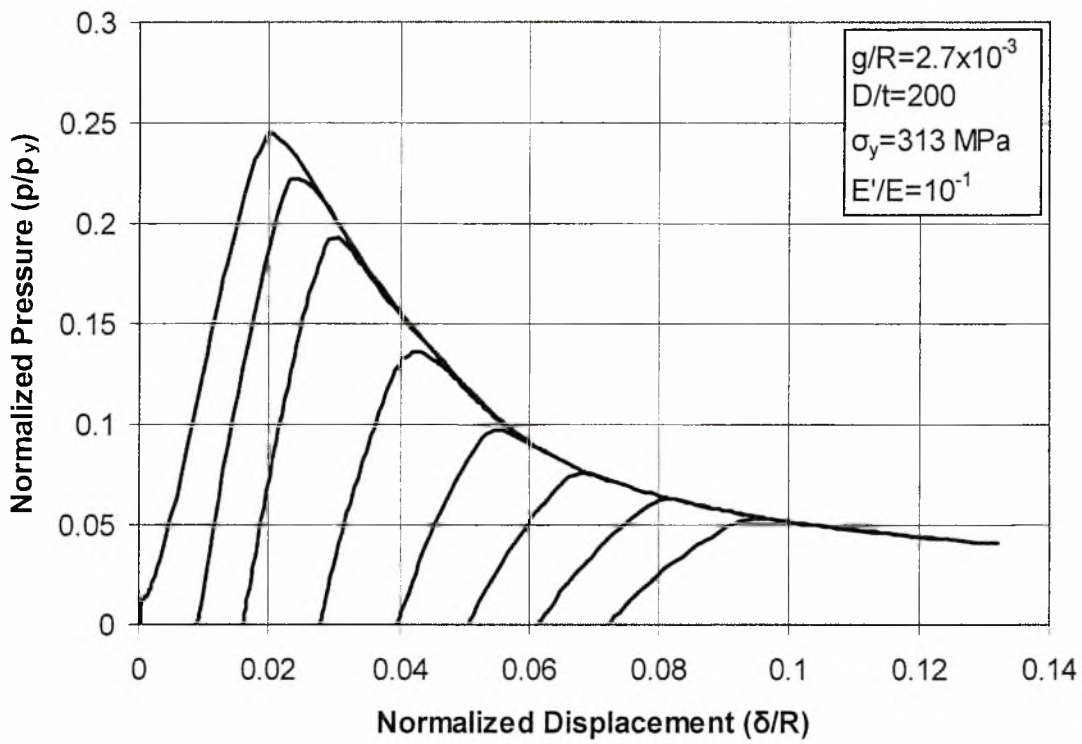

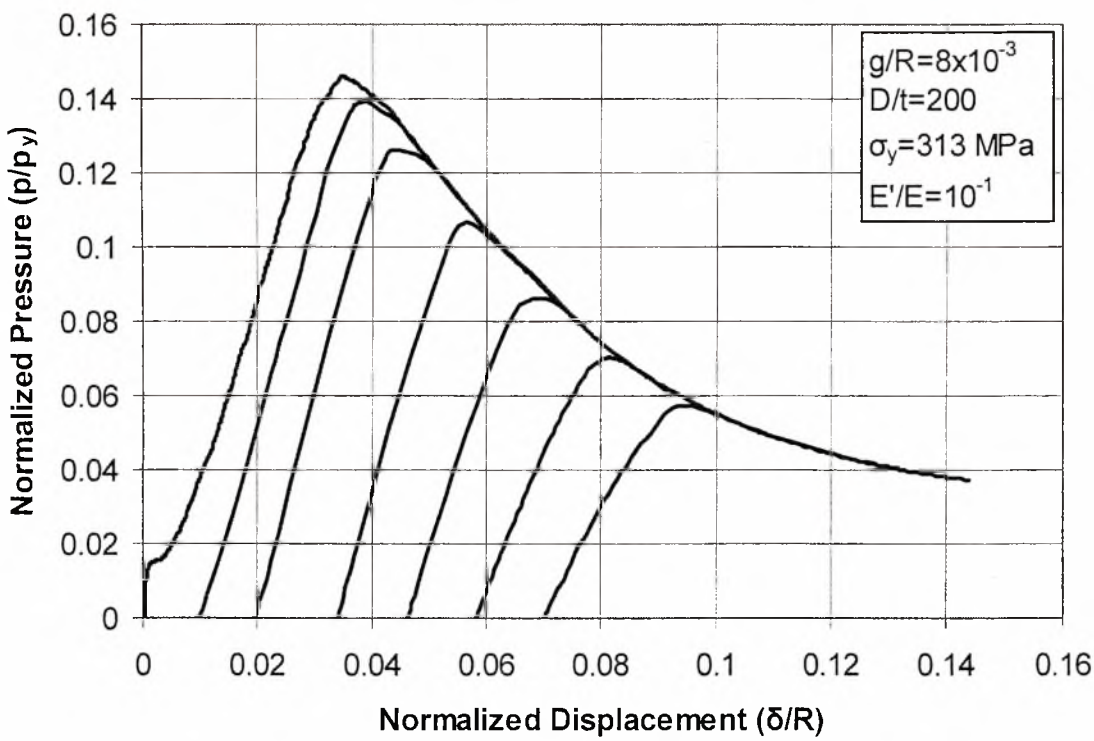

Figures 9 Effects of initial imperfection and initial gap on the external pressure response of a confined steel cylinder embedded in a rigid confinement medium ($E'/E = 10^{-1}$, $D/t = 200$).

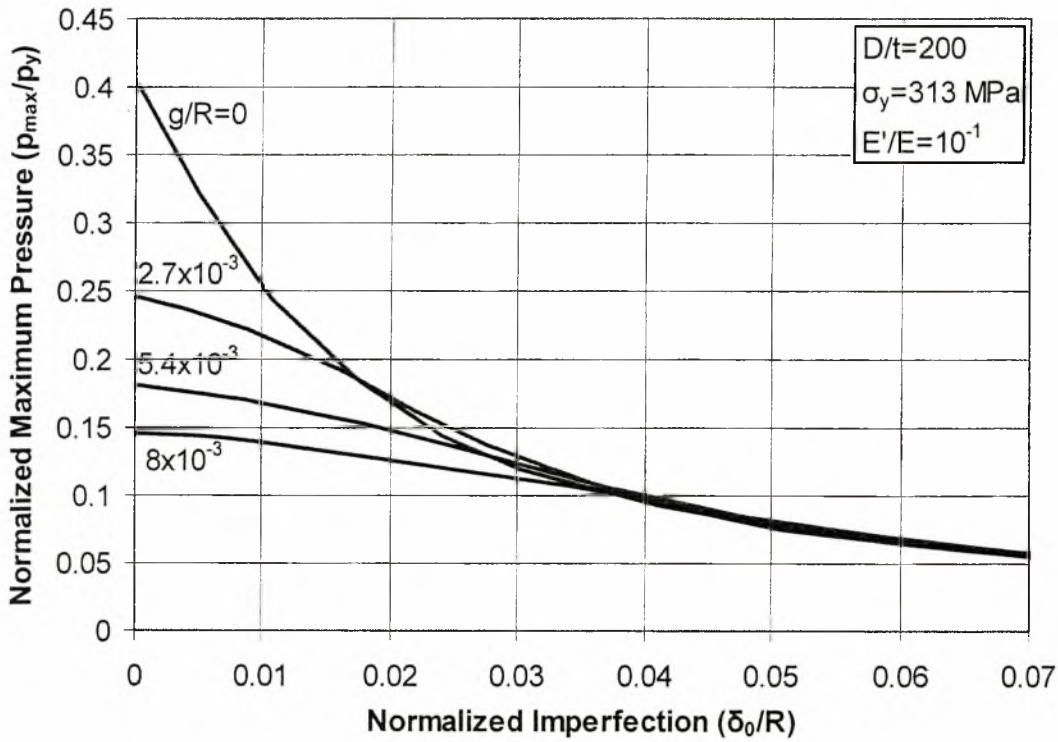

Figure 10 Effects of initial imperfection and initial gap (g/R) on the maximum pressure sustained by a confined steel cylinder embedded in a rigid confinement medium ($E'/E = 10^{-1}$, $D/t = 200$).

Figure 11 refers to the initial cylinder response, i.e. under low levels of external pressure, for three different values of initial gap size ($g/R = 0$, $g/R = 2.7\times10^{-3}$, $g/R = 8\times10^{-3}$). The pressure-displacement path for the two cases with nonzero initial gap is characterized by an abrupt change of slope at pressure level near $p/p_y = 0.016$, which corresponds to the critical buckling pressure p_e for elastic cylinders, calculated from equation (1.1). At this pressure level the cylinder buckles in an oval form (e.g. [1]). Upon buckling, the cylinder very quickly accommodates itself within the confinement boundary, and is able to sustain significant further increase of external pressure. This is represented by the increase of pressure in all three cases, beyond the critical pressure level ($p/p_y = 0.016$). The smaller the gap size, the sooner the pressure

increases. Under those conditions, a part of the cylinder behaves similar to an arch subjected uniform external pressure, supported at the two "touchdown" points B and B'. This leads to the so-called "inversion buckling", characterized by a limit-point on the pressure-deformation equilibrium path. The numerical results show that the maximum pressure $p_{\max}$ at the limit point occurs soon after first yielding of the cylinder wall. Furthermore, the response of the cylinder beyond the limit point is unstable, characterized by a significant drop of pressure, similar to the case of buckled arches [30].

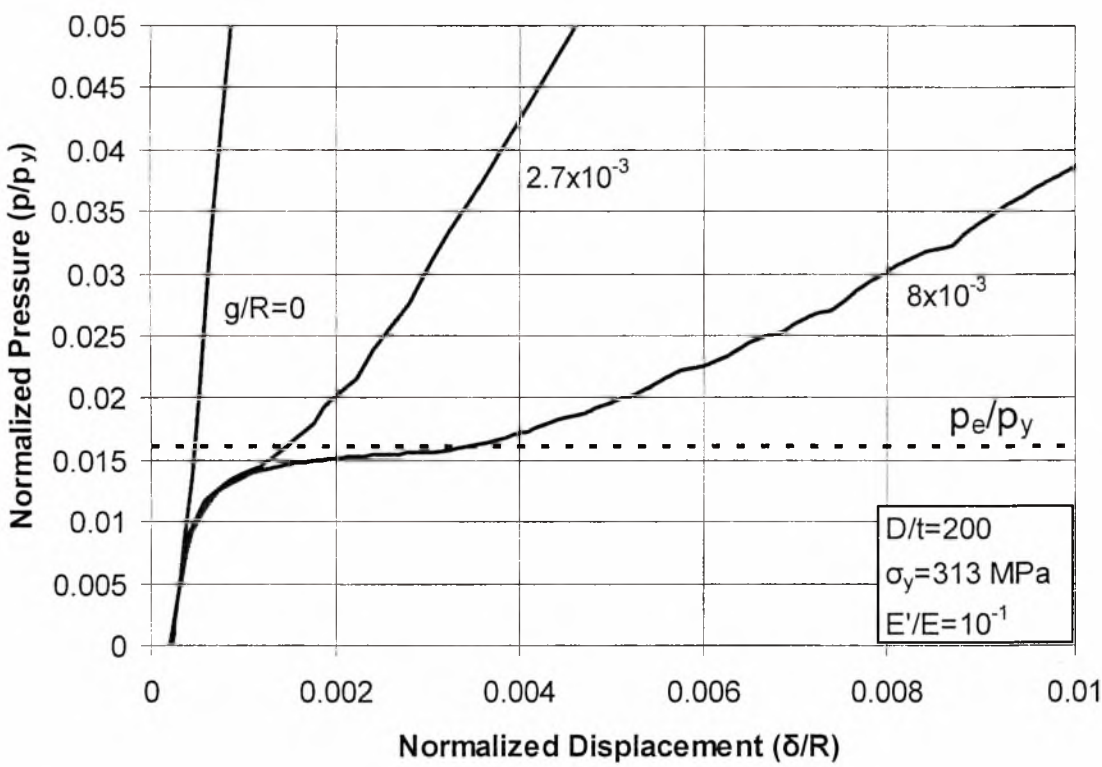

Figure 11 External pressure response of confined steel cylinders with different values of initial gap (g/R) embedded in a rigid confinement medium ($E'/E = 10^{-1}$, $D/t = 200$); low pressure levels.

Figure 12 shows the response of a thicker steel cylinder ($D/t = 100$) under external pressure, confined within a stiff boundary. The response is similar to the one presented in Figure 6 for the thin-walled cylinder with $D/t = 200$. However, the ultimate pressure p_{max} for the thicker cylinder ($D/t = 100$) is higher than the ultimate pressure of the thin-walled cylinder ($D/t = 200$). On the other hand, p_{max} is still lower than the plastic pressure of the cylinder p_y, even in the absence of initial imperfections and initial gap between the cylinder and the medium. The variation of ultimate pressure p_{max} with respect to initial imperfections is shown in Figure 13 for three values of D/t ratio (D/t =100, 150, 200) and for zero gap between the cylinder and the medium. The imperfection sensitivity is similar for all three cases, as indicated by the curves of Figure 13.

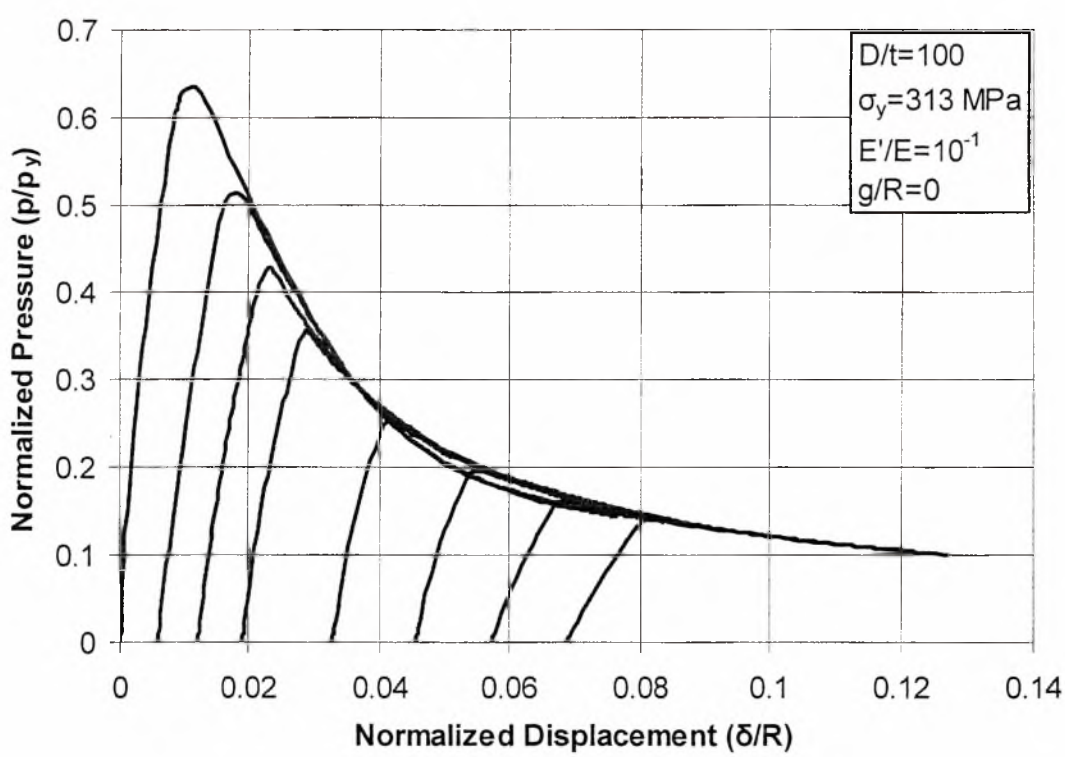

Figure 12 Response of tightly-fitted steel cylinders $(g/R = 0)$, embedded in a rigid confinement medium $(D/t = 100)$.

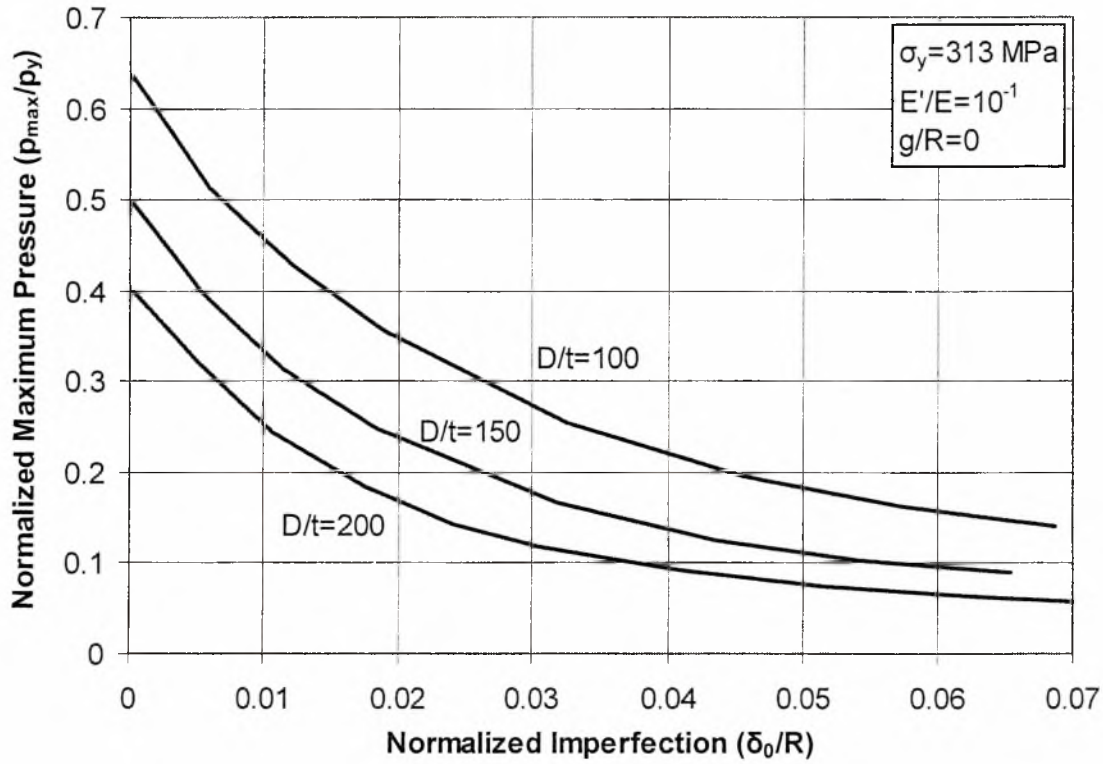

Figure 13 Effects of initial imperfection and D/t ratio on the maximum pressure sustained by a confined steel cylinder embedded in a rigid confinement medium ($E'/E=10^{-1}$, $g/R=0$).

The influence of medium deformability on the buckling response is shown in Figure 14, Figure 15 and Figure 16, for three values of E'/E ratio, equal to 10^{-3}, 10^{-4} and 3.3×10^{-5} respectively. The last value of medium stiffness E' corresponds to rather loose sand [31]. The results indicate that there is a substantial reduction of the p_{max} value, due to the elastic deformation of the medium. This reduction is attributed to the more pronounced deformations of the confined steel cylinder within the soft medium, under moderate pressure levels.

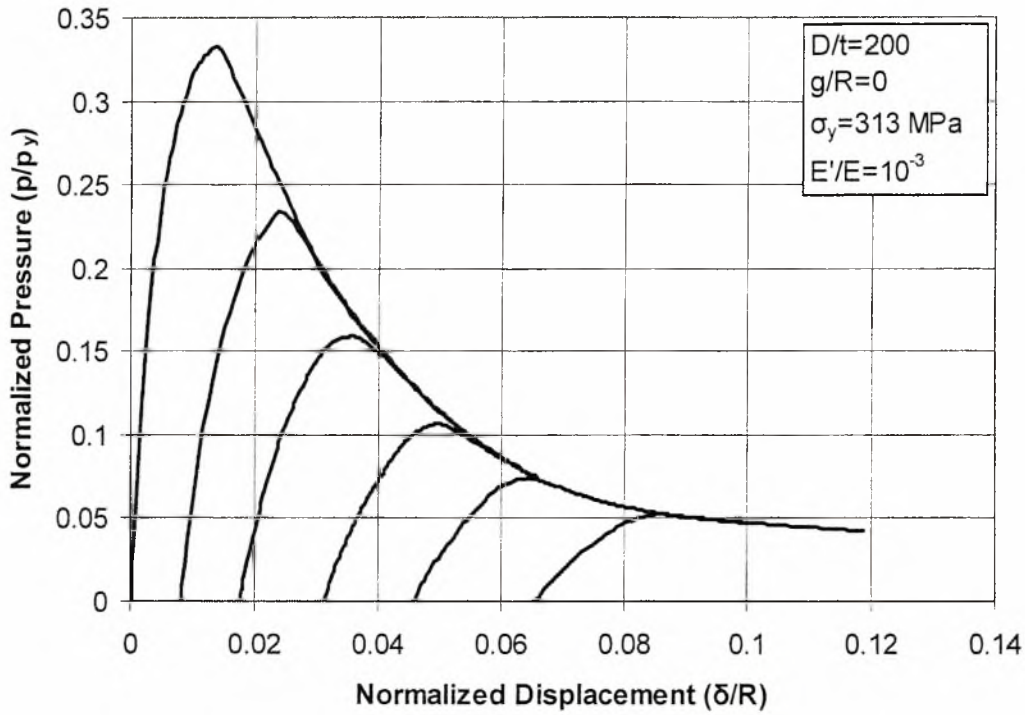

Figure 14 **Response of tightly-fitted steel cylinders $(g/R=0)$, embedded in a confinement medium with $E'/E=10^{-3}$ $(D/t=200)$.**

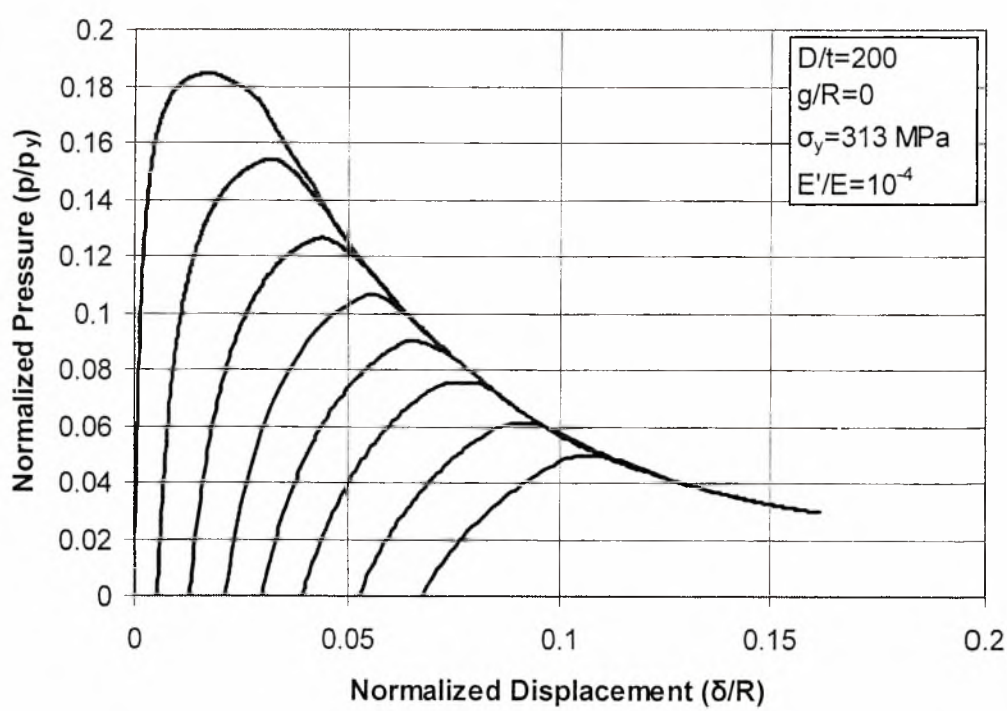

Figure 15 **Response of tightly-fitted steel cylinders $(g/R=0)$, embedded in a confinement medium with $E'/E=10^{-4}$ $(D/t=200)$.**

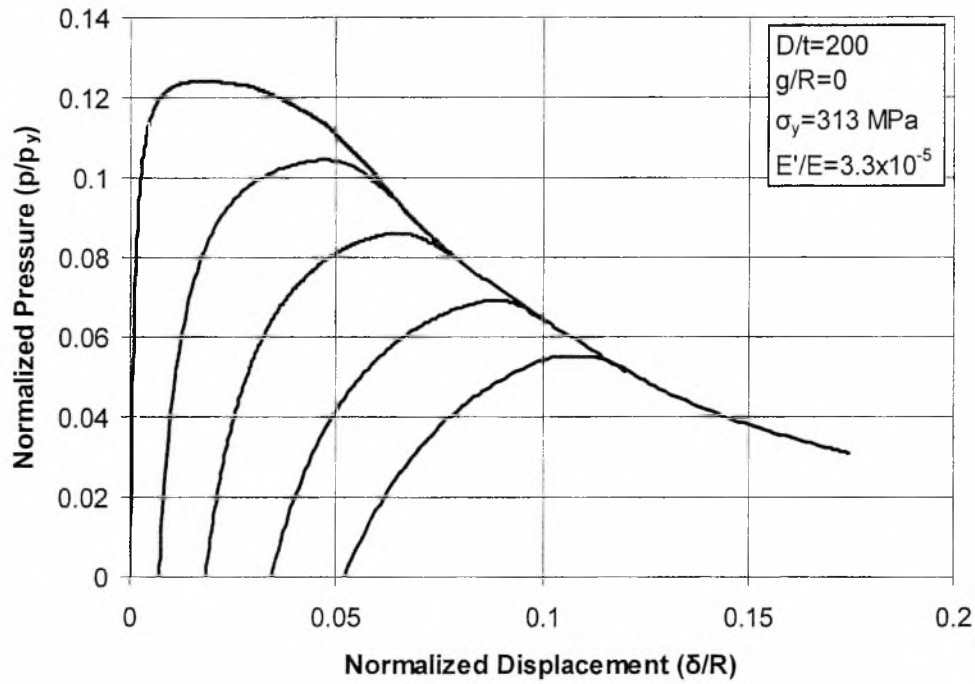

Figure 16 **Response of tightly-fitted steel cylinders $(g/R=0)$, embedded in a confinement medium with $E'/E=3.3\times10^{-5}$ $(D/t=200)$.**

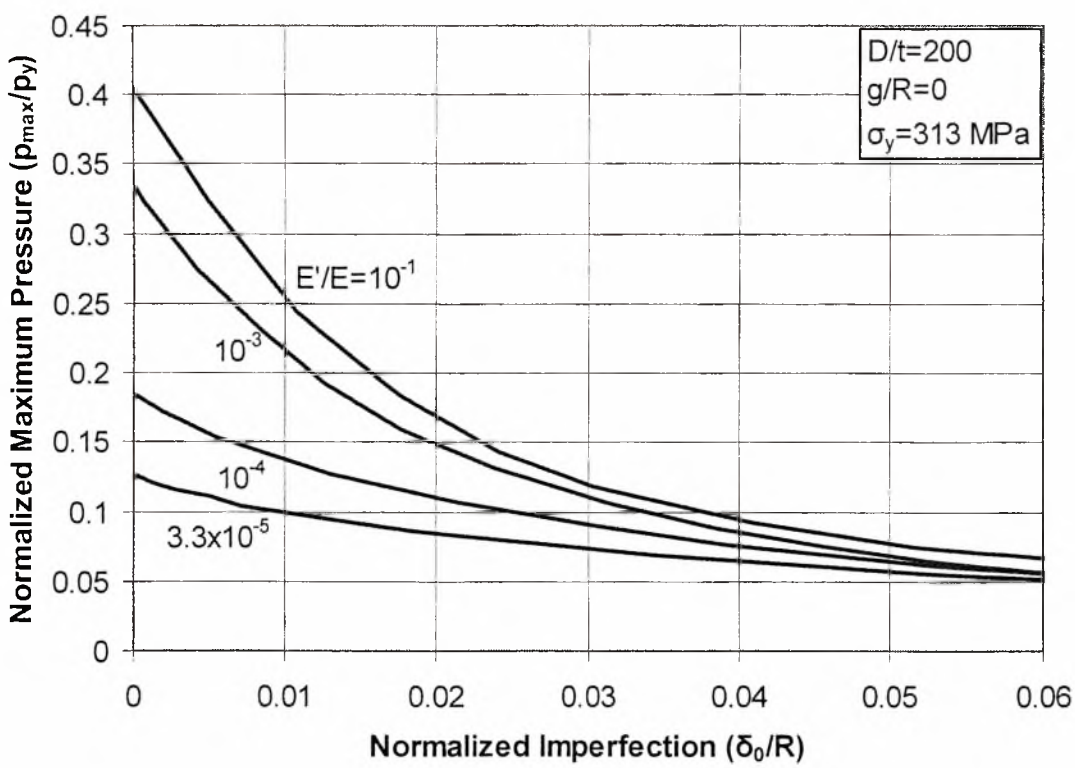

Figure 17 **Effects of initial imperfection and stiffness of confinement medium (E'/E) on the maximum pressure sustained by a confined steel cylinder ($g/R=0$, $D/t=200$).**

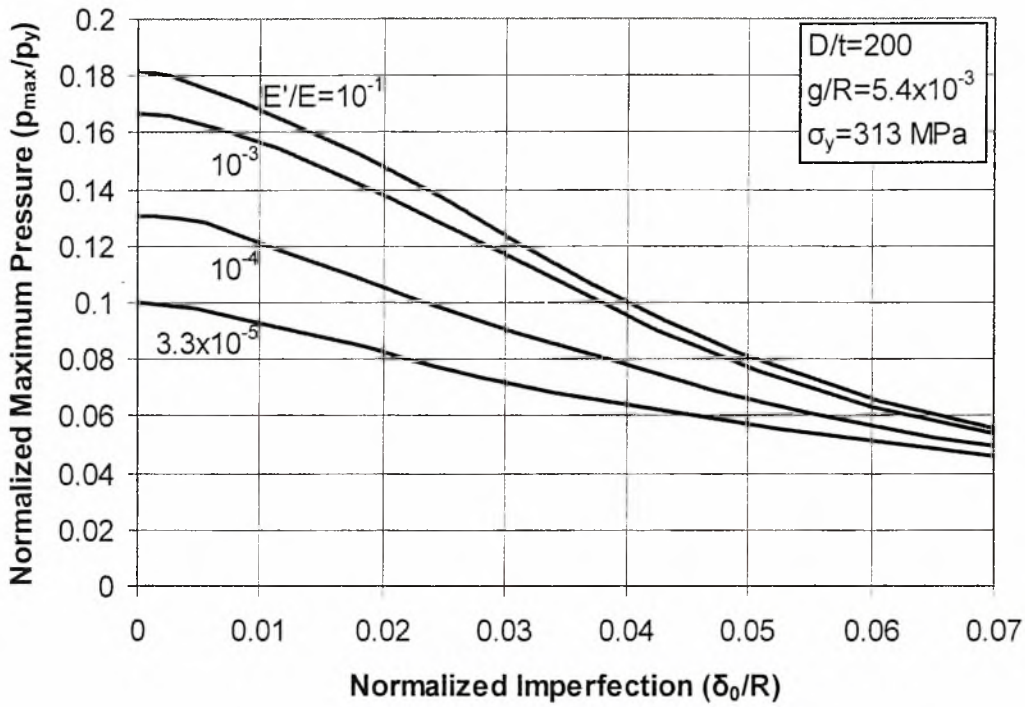

Figure 18 Effects of initial imperfection and stiffness of confinement medium (E'/E) on the maximum pressure sustained by a confined steel cylinder ($g/R = 5.4\times10^{-3}$, $D/t = 200$).

The variation of maximum pressure with respect to initial imperfection for four different values of the confinement medium modulus E' is plotted in Figure 17 and in Figure 18 for zero and non-zero gap respectively. The results in those Figures show that the imperfection sensitivity is quite significant for stiff confinement medium ($E'/E = 10^{-1}$), but considerably smaller for "soft" confinement medium (small values of the E'/E ratio).

The contact pressure developed in the interface between the cylinder and the medium is depicted in Figure 19 in a graphical form for the case of a soft confinement modulus E' ($E'/E = 3.3\times10^{-5}$), whereas Figure 20 shows the numerical values of contact pressure at consecutive points. Note that the maximum contact pressure occurs at point A_2 (Figure 19), which is located at the "touchdown" area with maximum plastic deformation (see point B in Figure 8).

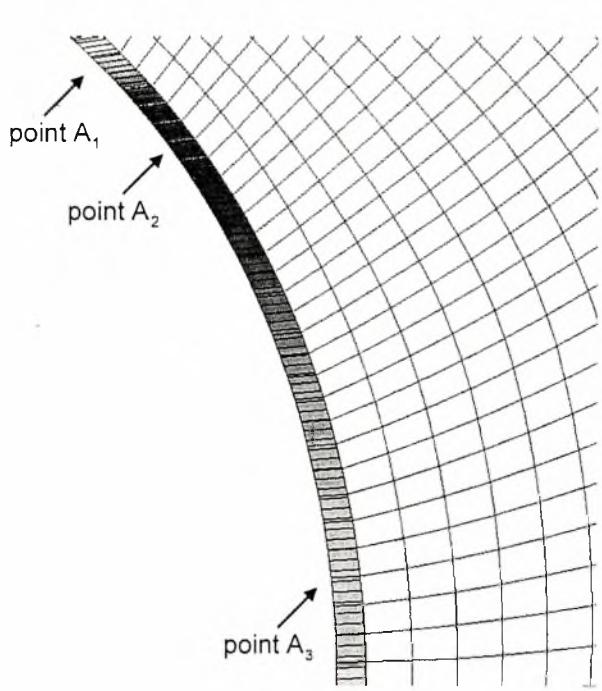

Figure 19 Graphical representation of contact pressure between the steel cylinder and the elastic medium ($E'/E = 3.3\times10^{-5}$, $D/t = 200$); maximum contact pressure occurs at point A_2.

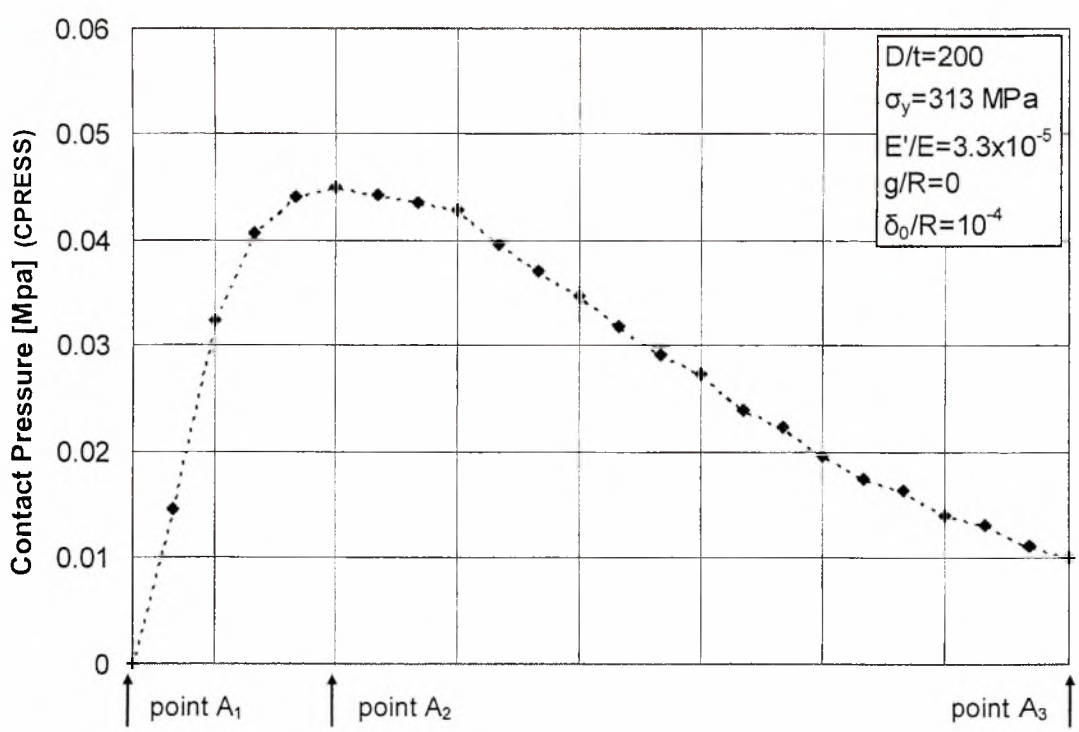

Figure 20 Variation of contact pressure between the steel cylinder and the elastic medium ($E'/E = 3.3\times10^{-5}$, $D/t = 200$).

Figures 21 show the effects of friction between the cylinder and the medium for two values of E'. Friction is considered through the friction coefficient μ, where $\mu = \tan\varphi$ and φ is the friction angle of the interface. In the present case, assuming a soil material with friction angle φ_s equal to 32°, the value of φ is considered equal to 10° and 16° (i.e. 1/3 and 1/2 of the value of φ_s), corresponding to μ values equal to 0.176 and 0.287 respectively. The numerical results show that consideration of friction results in a small increase of the ultimate capacity p_{max}. The friction effect is somewhat more pronounced in the case of soft confinement medium, whereas in the case of rigid confinement, this effect has been found to be negligible.

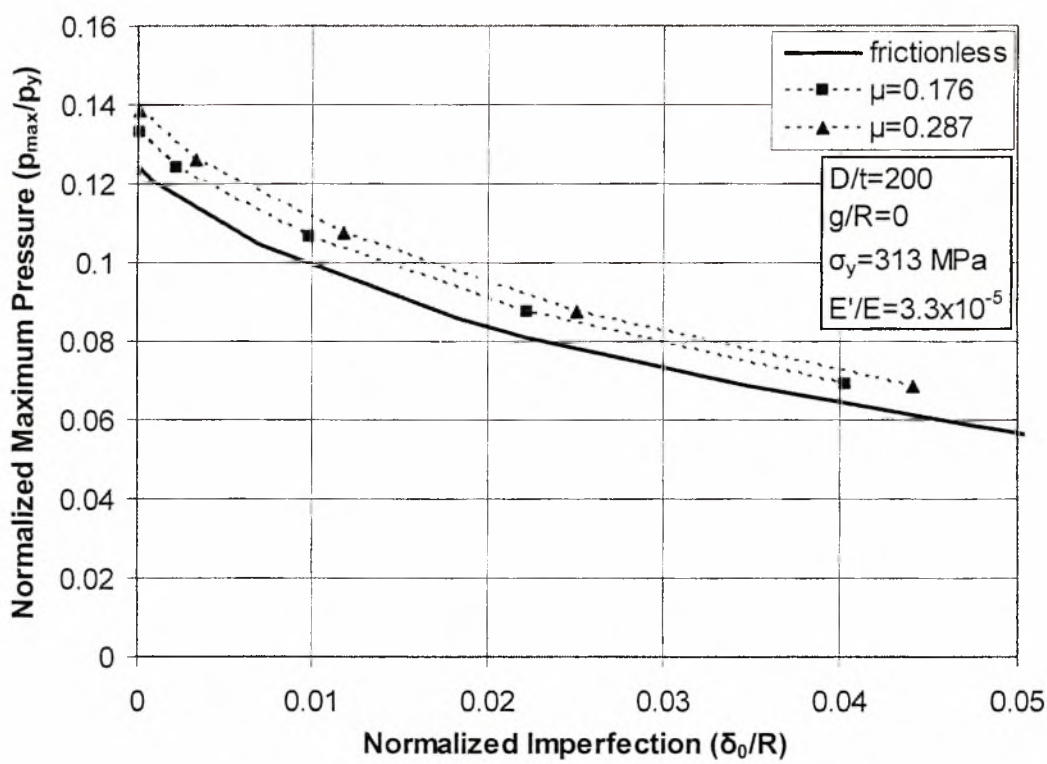

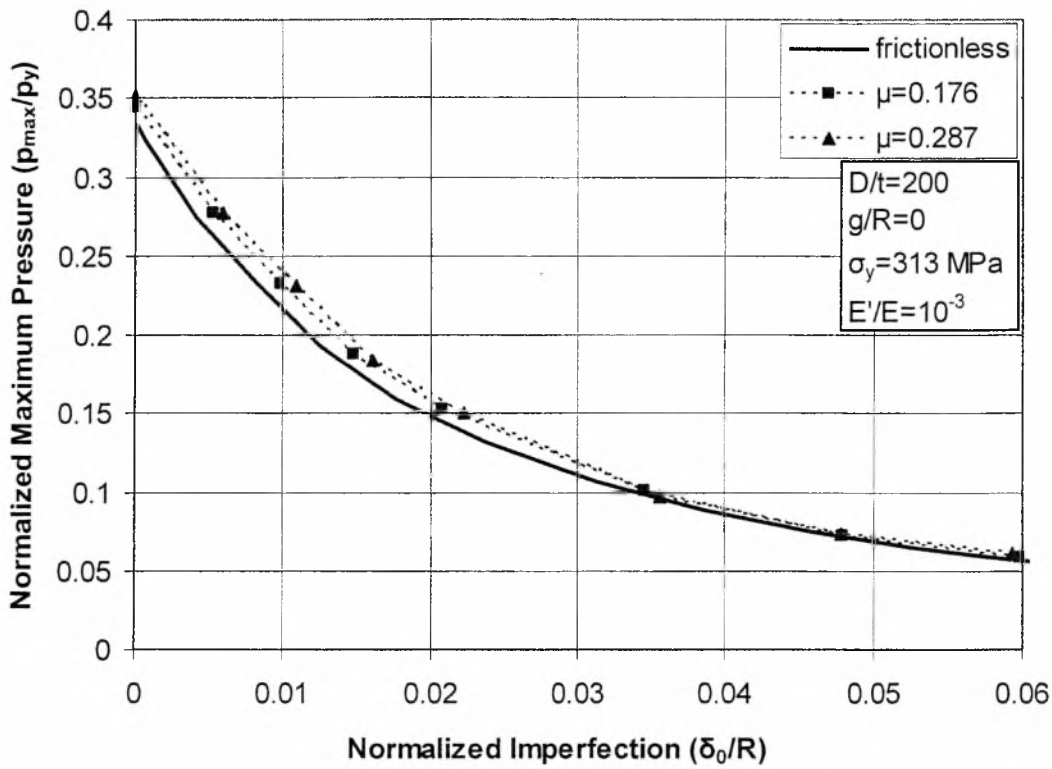

Figures 21 Effects of friction between the steel cylinder and the elastic confinement medium for $E'/E = 3.3\times10^{-5}$, and for $E'/E = 10^{-3}$ ($D/t = 200$).

The response of cylinders with different material properties are shown in Figures 22. When a stiff boundary is considered, the use of steel with higher yield strength results in an increase of the ultimate pressure $p_{\max}$. On the other hand, in the case of a soft confinement medium, the ultimate pressure seems to be rather insensitive to the value of yield stress. In such a case, value of $p_{\max}$ is quite small, due to the small contribution of the surrounding medium. In all three cases, buckling occurs in the elastic range and, therefore, yielding of steel material occurs after a maximum pressure occurs. The results of Figures 22 are also depicted in Figures 23 in a dimensionless form.

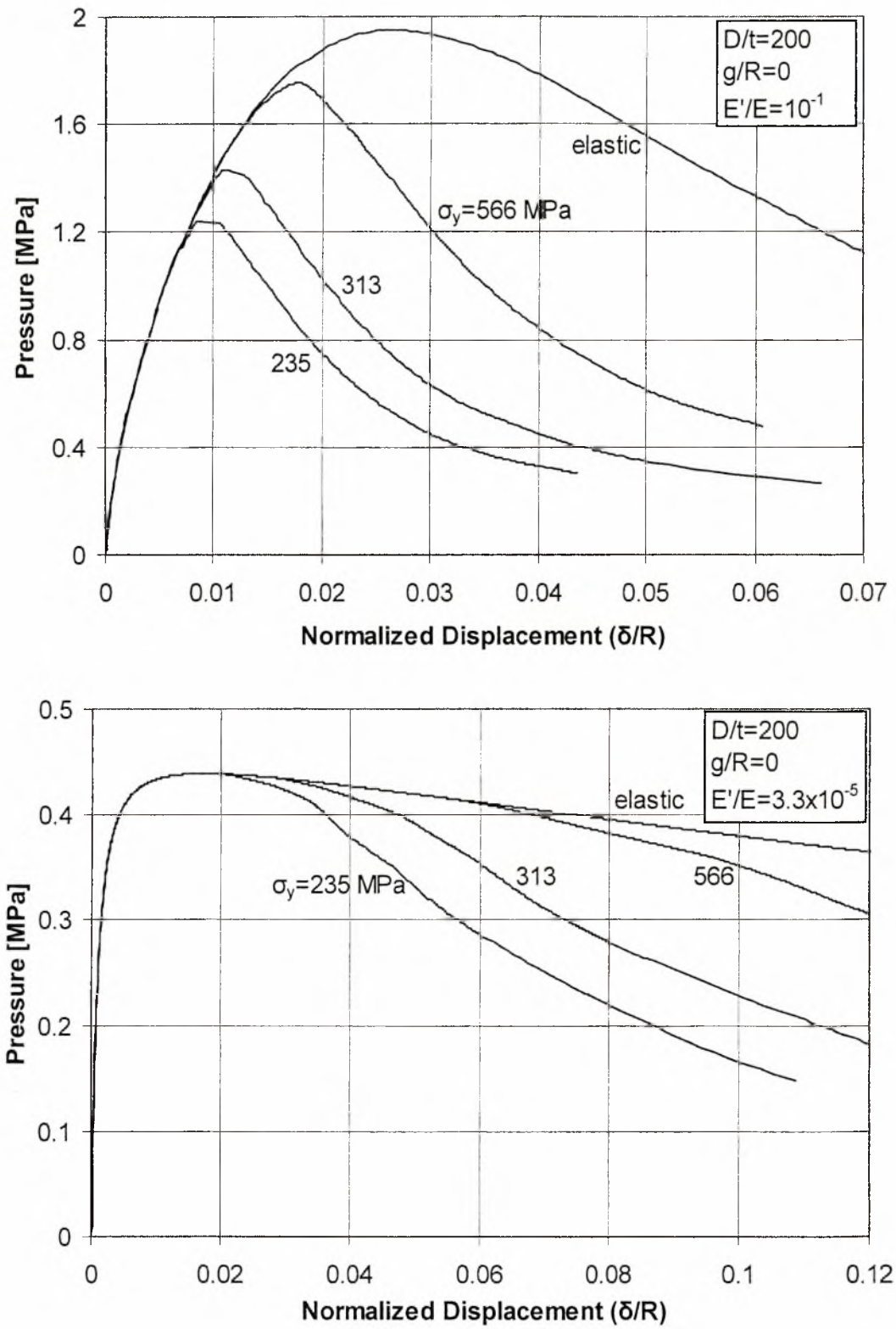

Figures 22 Response of steel cylinders ($g/R=0$), embedded in a confinement medium for $E'/E=10^{-1}$ and for $E'/E=3.3\times10^{-5}$ ($D/t=200$); pressure in [MPa] versus normalized deflection.

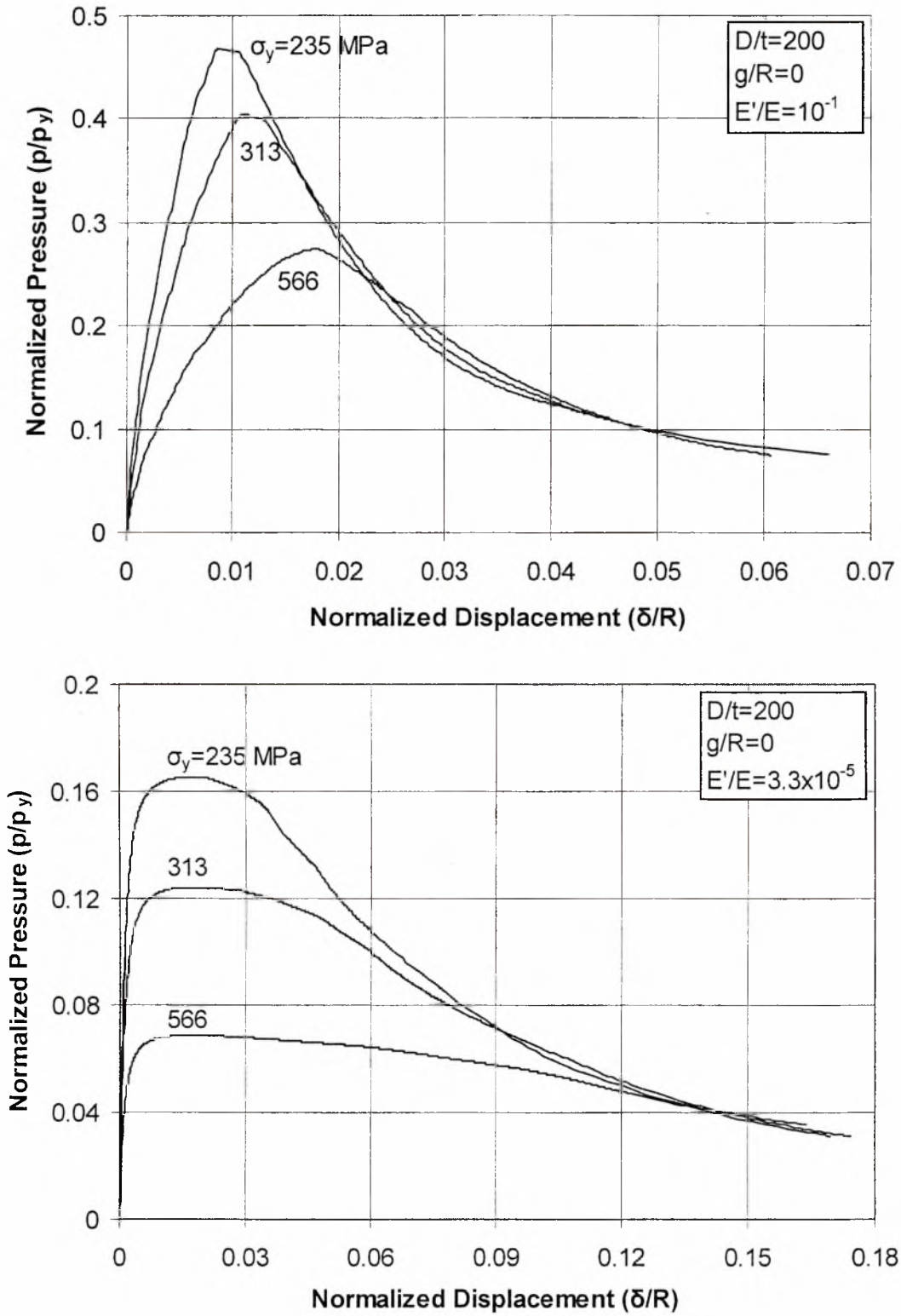

Figures 23 Normalized response of steel cylinders ($g/R=0$), embedded in a confinement medium for $E'/E=10^{-1}$ and for $E'/E=3.3\times10^{-5}$ ($D/t=200$); normalized pressure versus normalized deflection.

The effect of vertical preloading on the medium-cylinder system is shown in Figure 24 and Figure 25. Pre-loading is considered in the form of a vertical pressure q on the top edge of the medium, which is applied first and it is kept constant while the external pressure is increased. The values of q loading from overlying soil in a buried pipeline of height that ranges between 0 and 15 meters, assuming a unit weight of soil equal to $15 kN/m^3$. The values of vertical pressure q are normalized by the quantity $q_0 = \sigma_y (t/R)^2$ $\left(q^* = q/q_0\right)$. The numerical results show that, in the case of soft medium, preloading has a beneficial effect on the pressure capacity of the cylinder. On the other hand, negligible effect on the response has been observed in the case of a stiff medium.

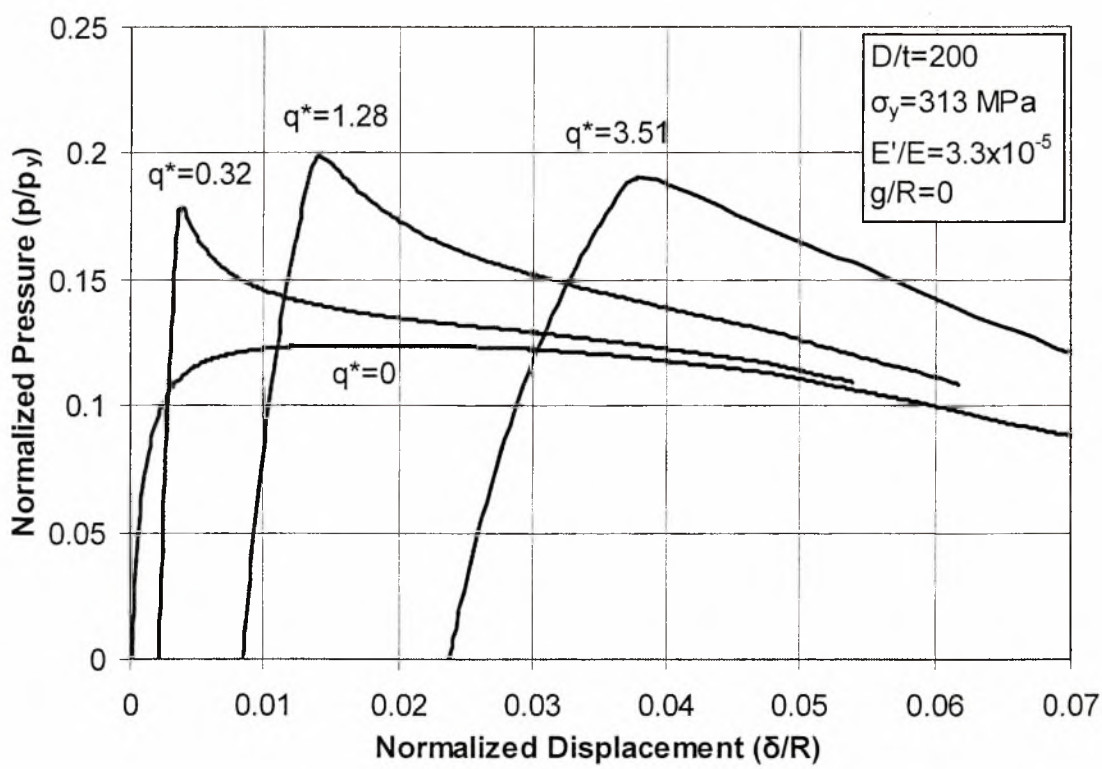

Figure 24 Effects of uniform preloading at the top of the surrounding medium, on pressure response of embedded steel cylinders.

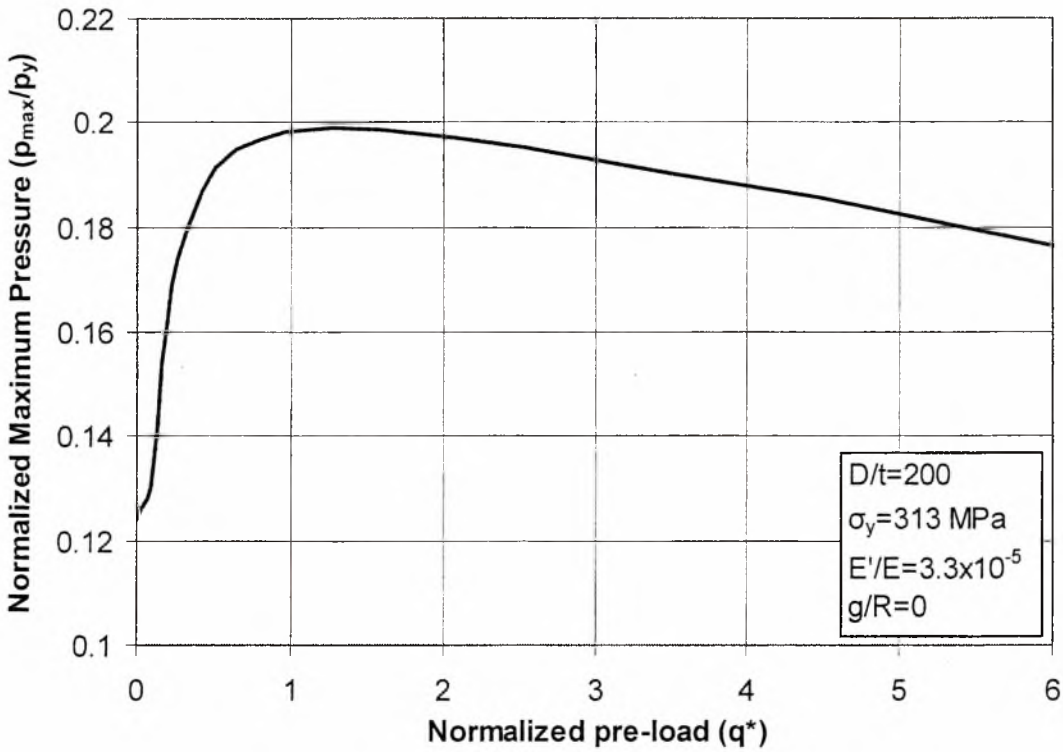

Figure 25 Variation of maximum pressure p_{max} sustained by the cylinder in the presence of pre-loading at the top of the surrounding medium ($E'/E = 3.3\times10^{-5}$, $D/t = 200$).

Finally, the predictions of equation (1.6) proposed by Montel [18] are compared with the present finite element results in Figure 26. The comparison shows that, despite its simplicity, the empirical formula (1.6) can provide reliable, yet somewhat conservative estimates of the maximum pressure sustained by the cylinder in a stiff boundary within a good level of accuracy. It is interesting to note that the good predictions of equation (1.6) are beyond the applicability ranges specified in the publication of Montel [18] and, therefore, the formula can be used for the design of buried pipelines encased in concrete or other cylinders confined within a stiff medium.

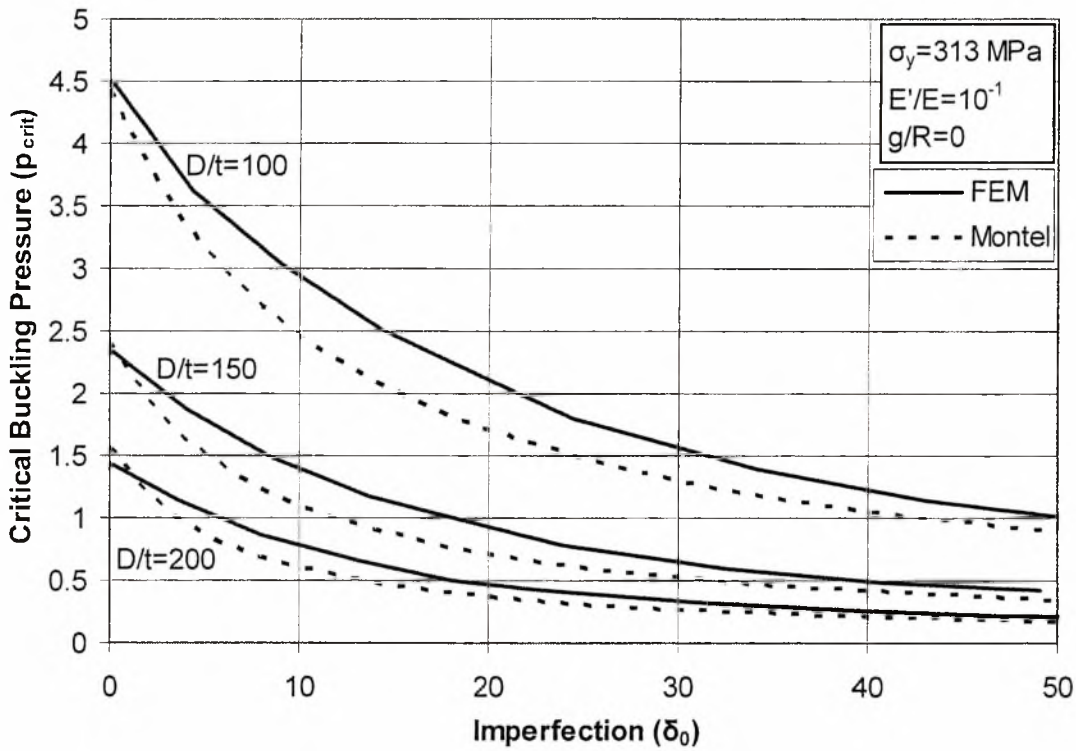

Figure 26 Comparison between numerical results and analytical predictions from Montel's simplified equation [18].

CHAPTER 5

CONCLUSIONS

The behavior of thin-walled steel cylinders, surrounded by an elastic medium, is examined in terms of their structural stability under uniform external pressure using a nonlinear two-dimensional finite element model. Numerical results on cylinders of elastic material are found to be in very close agreement with available closed-form analytical predictions. Subsequently, confined thin-walled steel cylinders $(100 \leq D/t \leq 200)$ are analyzed under external pressure. The numerical results show a significant sensitivity of the ultimate pressure in terms of initial out-of-roundness of the cylinder and the presence of initial gap between the cylinder and the medium. It is also demonstrated that reduction of the medium modulus results in a substantial reduction of the pressure capacity of the cylinder. Furthermore, the vertical preloading of the medium results in a pronounced increase of the ultimate pressure sustained by the cylinder. The pressure-deflection equilibrium paths indicate a rapid drop of pressure capacity after reaching the maximum pressure level, and the post-buckling configuration is characterized by a three-hinge plastic collapse mechanism, with one stationary and two moving plastic hinges. The maximum contact pressure between the cylinder and the medium occurs at the vicinity of the moving hinges. Finally, the simplified formula proposed by Montel [18] is found to be in good agreement with the present numerical results and could be used for the prediction of buckling pressure of buried pipelines and other rigidly encased steel cylinders.

REFERENCES

[1] Brush, D. O., Almroth, B. O. (1975). *Buckling of Bars, Plates, and Shells,* McGraw-Hill, New York, NY.

[2] American Petroleum Institute (1999). *Design, Construction, Operation and Maintenance of Offshore Hydrocarbon Pipelines (Limit State Design),* API RP 1111, 3rd edition, Washington, DC.

[3] Det Norske Veritas (2000). *Design Rules for Submarine Pipelines,* DNV-OS-F101, Oslo, Norway.

[4] American Petroleum Institute (1993). *Recommended Practice for Planning, Designing and Constructing Fixed Offshore Platforms,* API RP2A-LRFD, 1st edition, Washington, DC.

[5] Watkins, R. K. (2004). "Buried Pipe Encased in Concrete.", *International Conference on Pipeline Engineering & Construction,* ASCE, San Diego, CA.

[6] Omara, A. M., et al. (1997). "Buckling Models of Thin Circular Pipes Encased in Rigid Cavity.", *Journal of Engineering Mechanics,* ASCE, Vol. 123, No. 12, pp. 1294-1301.

[7] Ullamn, F. (1964). "External Water Pressure Designs for Steel-Lined Pressure Shafts.", *Water Power,* Vol. 16, pp. 298-305.

[8] Ahrens, T. (1970). "An In-Depth Analysis of Well Casings and Grouting: Basic Considerations of Well Design – II.", *Water Well Journal,* pp. 49-51.

[9] Hsu, P. T., et al. (1964). "Note on the Instability of Circular Rings Confined to a Rigid Boundary.", *Journal of Applied Mechanics,* ASME, Vol. 31, No. 3, pp. 559-562.

[10] Chicurel, R. (1968). "Shrink Buckling of Thin Circular Rings.", *Journal of Applied Mechanics,* ASME, Vol. 35, pp. 608-610.

[11] Bucciarelli Jr., L. L. and Pian, T. H. H. (1967). "Effect of Initial Imperfections on the Instability of a Ring Confined in an Imperfect Rigid Boundary.", *Journal of Applied Mechanics,* ASME, Vol. 34, No. 4, pp. 979-984.

[12] El-Bayoumy, L. (1972). "Buckling of a Circular Elastic Ring Confined to a Uniformly Contracting Circular Boundary.", *Journal of Applied Mechanics,* ASME, Vol. 39, No. 3, pp. 758-766.

[13] Soong, T. C. and Choi, I. (1985). "Buckling of an Elastic Elliptical Ring Inside a Rigid Boundary.", *Journal of Applied Mechanics,* ASME, Vol. 52, pp. 523-528.

[14] Cheney, J. A. (1971). "Pressure Buckling of Ring Encased in Cavity.", *Journal of Engineering Mechanics,* ASCE, Vol. 97, No. 2, pp. 333-342.

[15] Glock, D. (1977). "Uberkritisches Verhalten eines Starr Ummantelten Kreisrohres bei Wasserdrunck von Aussen und Temperaturdehnung." (Post-Critical Behavior of a Rigidly Encased Circular Pipe Subject to External Water Pressure and Thermal Extension), *Der Stahlbau,* Vol. 7, pp. 212-217.

[16] El-Sawy, K. and Moore, I. D. (1998). "Stability of Loosely Fitted Liners Used to Rehabilitate Rigid Pipes.", *Journal of Structural Engineering,* ASCE, Vol. 124, No. 11, pp. 1350-1357.

[17] Boot, J. C. (1998). "Elastic Buckling of Cylindrical Pipe Linings with Small Imperfections Subject to External Pressure.", *Trenchless Technology Research,* Vol. 12, No. 1-2, pp. 3-15.

[18] Montel, R. (1960). "Formule Semi-Empirique pour la Determination de la Pression Exterieure Limite d'instabilite des Conduits Metalliques Lisses Noyees dans du Beton.", *La Houllie Blanche 5.,* pp. 560-568.

[19] Timoshenko, S. and Gere, J. M. (1961). *Theory of Elastic Stability*, Second Edition, McGraw-Hill, New York, NY.

[20] Amstutz, E. (1969). "Das Einbeulen von Schacht – und Stollenpanzerungen.", *Schweizerische Bauzeitung,* Vol. 87, pp. 541-549. (U.S. Dept. of the Interior, Translation No. 825).

[21] Jacobsen, S. (1974). "Buckling of Circular Rings and Cylindrical Tubes Under External Pressure.", *Water Power,* Vol. 26, pp. 400-407.

[22] Yamamoto, Y. and Matsubara, N. (1982). "Buckling of a Cylindrical Shell Under External Pressure Restrained by an Outer Rigid Wall.", *Proceedings, Symposium on Collapse and Buckling, Structures; Theory and Practice,* Cambridge University Press, London, U.K., pp. 493-504.

[23] Kyriakides, S. and Youn, S. K. (1984). "On the Collapse of Circular Confined Rings Under External Pressure.", *International Journal of Solids and Structures,* Vol. 20, No. 7, pp. 699-713.

[24] Kyriakides, S. (1986). "Propagating Buckles in Long Confined Cylindrical Shells.", *International Journal of Solids and Structures,* Vol. 22, No. 12, pp. 1579-1597.

[25] Kyriakides, S. and Lee, L.-H. (2005). "Buckle Propagation in Confined Steel Tubes.", *International Journal of Mechanical Sciences,* Vol. 47, No. 4-5, pp. 603-620.

[26] El-Sawy, K. (2001). "Inelastic Stability of Tightly Fitted Cylindrical Liners Subjected to External Uniform Pressure.", *Thin-Walled Structures,* Vol. 39, No. 9, pp. 731-744.

[27] El-Sawy, K. (2002). "Inelastic Stability of Loosely Fitted Cylindrical Liners.", *Journal of Structural Engineering,* ASCE, Vol. 128, No. 7, pp. 934-941.

[28] Hibbit, H. D., Karlsson, B. I. and Sorensen, P. (2005). *Theory Manual,* ABAQUS, version 6.4, Providence, RI, USA.

[29] Aggarwal, S. C. and Cooper, M. J. (1984). "External Pressure Testing of Insituform Lining.", *Internal Report,* Coventry (Lanchester) Polytechnic, Coventry, U.K.

[30] Bazant, Z. P. and Cedolin, L. (1991). *Stability of Structures, Elastic, Inelastic, Fracture and Damage Theories,* Oxford University Press, Oxford, U.K.

[31] Jeyapalan, J. K. and Watkins, R. K. (2004). "Modulus of Soil Reaction (E') Values for Pipeline Design.", *Journal of Transportation Engineering,* ASCE, Vol. 130, No. 1, pp. 43-48.

APPENDIX

Summary of Glock's analytical solution [15]

Glock [15] presented a solution for external pressure buckling of elastic rings confined with a rigid medium. The kinematics were based on the Donnell approximations of thin-ring equations [1]. More specifically, the total hoop axial strain is given by the following equation:

$$\varepsilon_\theta = \varepsilon_m + kz \tag{1.1}$$

where the membrane and bending strain are given in terms of the radial and tangential displacements v and w of the ring reference line at mid-thickness as follows

$$\varepsilon_m = \frac{1}{R}\left(v' - w\right) + \frac{1}{R}w'^2 \tag{1.2}$$

$$k = \frac{w''}{R^2} \tag{1.3}$$

Ring deformation consists of two parts, the "buckled" region and the "unbuckled" region (Figure 27). An assumed shape function $w(\theta)$ for the buckled region is assumed as follows

$$w(\theta) = \delta \cos^2\left(\frac{\pi\theta}{2\phi}\right) \tag{1.4}$$

where ϕ is the angle that defines the border between the "buckled" and the "unbuckled" ring portions, so that $-\phi \le \theta \le \phi$.

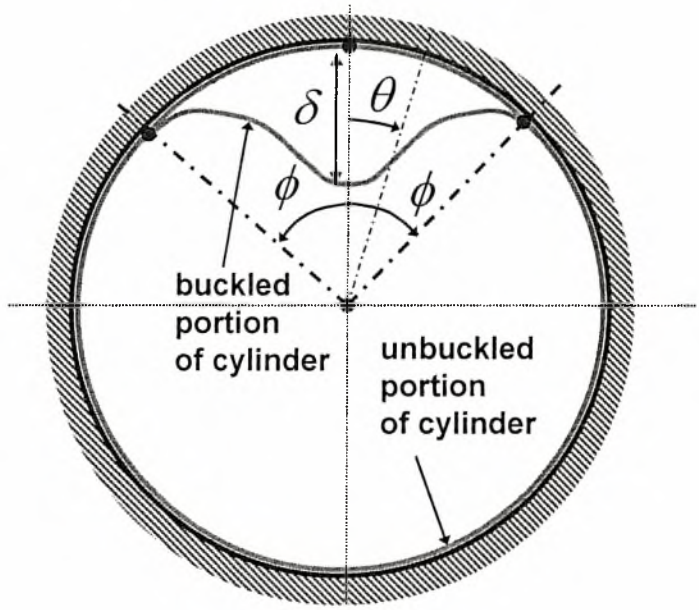

Figure 27 Schematic representation of Glock's model [15]; the cylinder is divided in two parts, a buckled portion and an unbuckled portion.

Forming the total potential energy Π of the ring, assuming a constant hoop axial force N_{ave} around the ring, and requiring minimization of Π with respect to both δ and ϕ, closed-form expressions for the pressure p, the amplitude of buckled shape δ and the axial force N are obtained in terms of angle ϕ:

$$\frac{\delta}{R} = -\frac{6pR^3}{EI}\left(\frac{\phi}{\pi}\right)^4 + 10\left(\frac{\phi}{\pi}\right)^2 \tag{1.5}$$

$$\frac{pR^3}{EI} = \left(\frac{\pi}{\phi}\right)^2\left[1 \pm \frac{1}{6}\sqrt{16 - \frac{80}{3}\left(\frac{EI}{EAR^2}\right)\left(\frac{\pi}{\phi}\right)^5}\right] \tag{1.6}$$

$$N = \frac{5}{3}\frac{EI}{R^2}\left(\frac{\pi}{\phi}\right)^2 \tag{1.7}$$

Subsequently, minimization of pressure in terms of angle ϕ, results in final closed form expressions for the critical pressure p_{GL}, the corresponding angle ϕ_{cr}, and the corresponding amplitude of the buckling shape:

$$\frac{p_{GL}R^3}{EI} = 0.969\left(\frac{EAR^2}{EI}\right)^{2/5} \tag{1.8}$$

$$\left(\frac{\pi}{\phi}\right)_{cr} = 0.856\left(\frac{EAR^2}{EI}\right)^{1/5} \tag{1.9}$$

$$\left(\frac{\delta}{R}\right)_{cr} = 2.819\left(\frac{EI}{EAR^2}\right)^{2/5} \tag{1.10}$$

For the case of a ring under plane-strain conditions, equation (1.8) can be written in the form of equation (1.4) of Chapter 1.